nature chemical biology

ARTICLES

https://doi.org/10.1038/s41589-020-0639-1

Optogenetic control of the *lac* operon for bacterial chemical and protein production

Makoto A. Lalwani[1], Samantha S. Ip[1,4], César Carrasco-López[1,4], Catherine Day[2], Evan M. Zhao[1], Hinako Kawabe[1] and José L. Avalos[1,2,3] ✉

Control of the *lac* operon with isopropyl β-D-1-thiogalactopyranoside (IPTG) has been used to regulate gene expression in *Escherichia coli* for countless applications, including metabolic engineering and recombinant protein production. However, optogenetics offers unique capabilities, such as easy tunability, reversibility, dynamic induction strength and spatial control, that are difficult to obtain with chemical inducers. We have developed a series of circuits for optogenetic regulation of the *lac* operon, which we call OptoLAC, to control gene expression from various IPTG-inducible promoters using only blue light. Applying them to metabolic engineering improves mevalonate and isobutanol production by 24% and 27% respectively, compared to IPTG induction, in light-controlled fermentations scalable to at least two-litre bioreactors. Furthermore, OptoLAC circuits enable control of recombinant protein production, reaching yields comparable to IPTG induction but with easier tunability of expression. OptoLAC circuits are potentially useful to confer light control over other cell functions originally designed to be IPTG-inducible.

The long history of *Escherichia coli* as a model organism makes it a preferred host for many biotechnological applications, including metabolic engineering and recombinant protein production. The abundance of genetic tools and wealth of knowledge about its physiology, genetics and metabolism have made *E. coli* an organism of choice across the spectrum of metabolic engineering, from proofs of principle[1] to large-scale industrial processes[2,3]. However, metabolic engineering in *E. coli* still faces important challenges that may be addressed with new technological improvements.

A key hurdle arises when engineered pathways cause cellular toxicity, metabolic burden or competition with cell growth, resulting in poor productivity. This can be addressed by dynamically controlling fermentations through a growth phase (in which engineered pathways are repressed to focus the cellular metabolism on biomass build-up) and a production phase (in which engineered pathways are induced for product biosynthesis)[4]. However, pathway productivities can be greatly impacted by the timing, rates and levels of induction, which can be difficult to control with chemical inducers. We recently showed that light can be an effective alternate inducing agent for metabolic engineering in *Saccharomyces cerevisiae*, enhancing dynamic control over fermentations by adding tunability, reversibility and independence from medium composition[5]. To achieve this, we devised optogenetic circuits that harness the galactose regulon, which is frequently utilized to induce gene expression in yeast.

The most commonly used inducible system in *E. coli* is based on the *lac* operon[6]. In the absence of lactose, the LacI repressor binds to *lac* operator (*lacO*) sites upstream of genes involved in lactose metabolism, repressing them. Allolactose binding to LacI causes it to dissociate from *lacO* sites, thus allowing gene transcription. For decades, this system has been exploited for dynamic control of gene expression in *E. coli*, using *lacO* sites to recruit LacI to a variety of promoters, and isopropyl β-D-1-thiogalactopyranoside (IPTG), a non-metabolizable allolactose mimetic, as an inducing agent[7]. These features of the *lac* operon provide an opportunity to develop optogenetic circuits to control gene expression in *E. coli* with light.

Several optogenetic systems have been developed in *E. coli*[8–10]. Among these, the photoreceptor signaling cascade encoded in the pDawn plasmid[10] seemed particularly adept at harnessing the *lac* operon. The pDawn system is derived from an engineered blue light-responsive photosensory histidine kinase YF1 and its cognate response regulator FixJ from *Bradyrhizobium japonicum*. In the dark, YF1 phosphorylates FixJ, which then activates the P_{FixK2} promoter to express the λ phage repressor cI. This repressor in turn prevents transcription from its cognate P_R promoter, which controls genes of interest. Conversely, blue light (~470 nm) induces YF1 phosphatase activity[11], thus reversing FixJ phosphorylation and cI expression. With this design, genes controlled by P_R are repressed in the dark by cI and expressed in blue light by the absence of this repressor.

Here we report optogenetic control of the *lac* operon using a series of circuits we call OptoLAC, in which *lacI* is controlled by the P_R promoter of the pDawn system. These optogenetic circuits bestow light controls on promoters originally designed to be IPTG-inducible. We show that OptoLAC circuits can replace IPTG with light to control engineered metabolic pathways for chemical production in up to lab-scale bioreactors, reaching titers of mevalonate and isobutanol that are higher than those achieved with IPTG induction. OptoLAC circuits are also functional in *E. coli* B strains to control recombinant protein production with light. OptoLAC circuits thus open the door to using light control not only for metabolic engineering and protein production in *E. coli*, but potentially also for other applications currently using IPTG.

Results

Optogenetic circuits to control the *lac* operon. To develop light controls for *E. coli*, we placed *lacI* under the cI-controlled P_R promoter

[1]Department of Chemical and Biological Engineering, Princeton University, Princeton, NJ, USA. [2]Department of Molecular Biology, Princeton University, Princeton, NJ, USA. [3]The Andlinger Center for Energy and the Environment, Princeton University, Princeton, NJ, USA. [4]These authors contributed equally: Samantha S. Ip, César Carrasco-López. ✉e-mail: javalos@princeton.edu

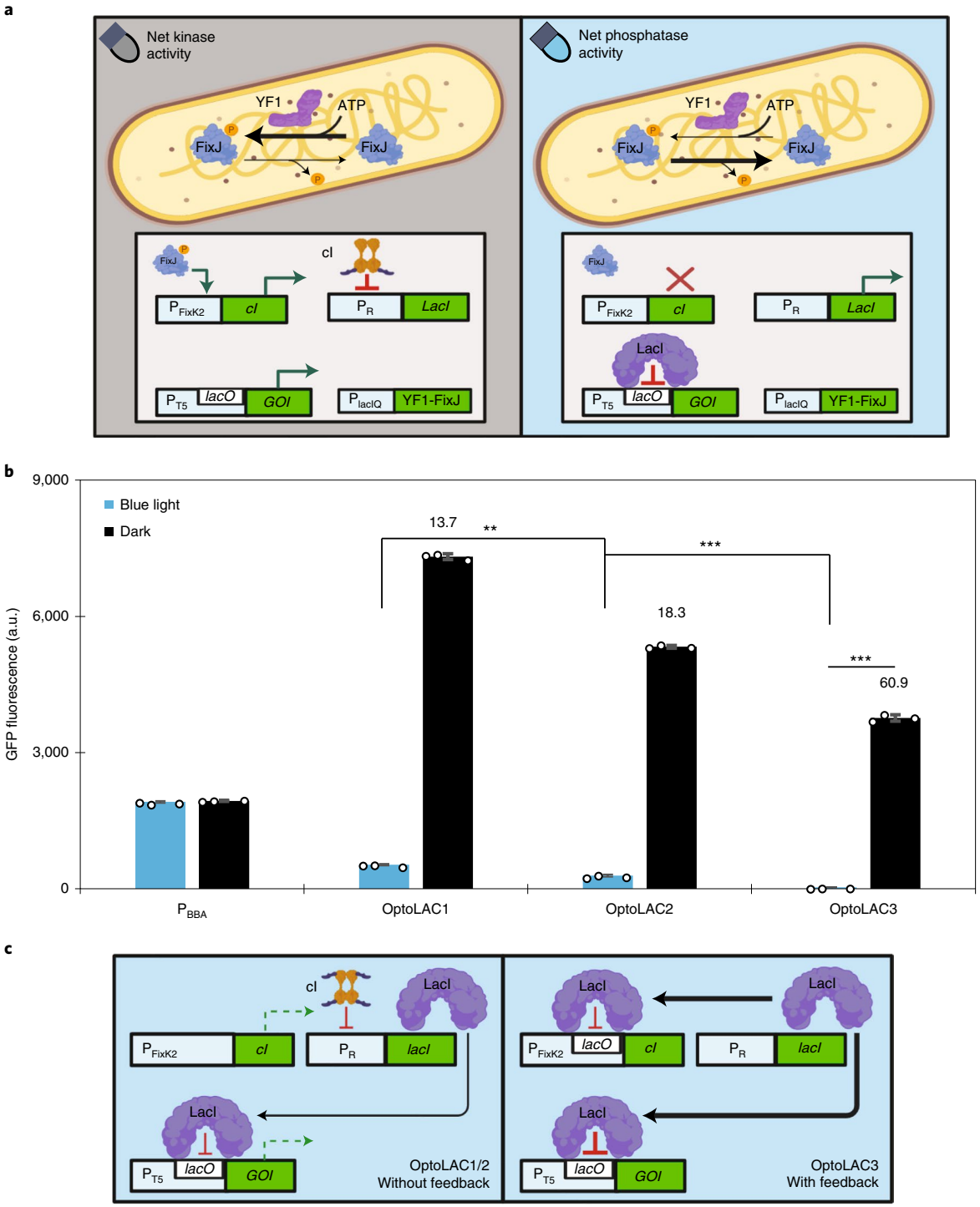

Fig. 1 | OptoLAC circuits design. a, OptoLAC circuits use the pDawn system to control *lacI* expression. Genes of interest (GOIs) controlled by *lacO*-containing promoters are repressed in blue light. **b**, GFP expression from P_{BBA} (EMAL231) or $P_{T5\text{-}lacO}$ controlled by OptoLAC1 (EMAL68), OptoLAC2 (EMAL69) or OptoLAC3 (EMAL230) in blue light (blue) or darkness (black). The fold of induction of each OptoLAC circuit is shown. From OptoLAC1 to OptoLAC3: $P = 0.00411$, $P = 0.000042$ and $P < 0.00001$. Significance of differences between light-repressed states: $^{**}P < 0.01$, $^{***}P < 0.001$. Statistics are derived using a two-sided *t*-test. All data are shown as median values of 10,000 single-cell flow cytometry events; error bars represent 1 s.d. of $n = 3$ biologically independent samples; open circles represent individual data points. Data are representative of $n = 3$ independent experiments. **c**, In contrast to the leakiness (dashed green arrow) of OptoLAC1 and OptoLAC2 (left panel), a *lacO* site downstream of P_{FixK2} in OptoLAC3 creates a positive feedback loop under blue light that tightens repression of GOIs (right panel). Panels **a** and **c** were created with Biorender.com.

of pDawn, such that genes of interest are repressed in the light and induced in the dark (Fig. 1a). To ensure control over total LacI levels, we transformed a Δ*lacI E. coli* K-12 MG1655 strain[12] (EMAL52, hereafter OptoMG) with plasmids to control *lacI* expression with pDawn (pMAL288; Supplementary Table 1), and superfolder green fluorescent protein (GFP) expression with the

IPTG-inducible promoter $P_{T5\text{-}lacO}$ (pMAL292), resulting in strain EMAL57 (Supplementary Table 2). Growing EMAL57 in either light or dark conditions results in no significant difference in GFP expression and less than 1% of the constitutive promoter P_{BBa_J23100} (P_{BBA}), (Extended Data Fig. 1a), indicating that pDawn control of *lacI* expression requires further engineering to achieve robust optogenetic control of gene expression.

The poor induction and overall low levels of GFP expression in EMAL57 suggest that levels of LacI in this strain are too high, regardless of cI activity. To address this, we reduced the half-life of LacI by fusing C-terminal degradation tags from the 10Sa transfer-messenger RNA (SsrA)[13] of different strength based on the last three amino acids[14]: SsrA-LAA (pMAL294), SsrA-AAV (pMAL296) or SsrA-ASV (pMAL300). Two of the three resulting strains (EMAL68, EMAL69 and EMAL71; Supplementary Table 2) show darkness-induced GFP expression levels that exceed constitutive expression from P_{BBA} (Extended Data Fig. 1b). Using the strongest SsrA-LAA tag results in the highest GFP expression in the dark. However, the SsrA-AAV tag offers tighter control of gene expression under blue light, probably due to higher LacI-mediated repression. We continued our study using LacI fusions to SsrA-LAA and SsrA-AAV, naming them OptoLAC1 (3.78-fold higher expression than P_{BBA}, with 13.7-fold induction) and OptoLAC2 (2.75-fold higher expression than P_{BBA}, with 18.3-fold induction), respectively (Fig. 1b).

Although fusing LacI to degradation tags improves GFP expression in the dark, it also increases basal expression in the light (Fig. 1b). To reduce the leakiness of OptoLAC2, we introduced a *lacO* operator sequence downstream of the P_{FixK2} promoter controlling cI expression (Supplementary Notes 1 and 2). With this design, LacI represses transcription of both the gene of interest (GOI; for example GFP) and the cI repressor that controls its own expression, creating a positive feedback loop that tightens circuit repression (Fig. 1c). This additional circuit, OptoLAC3 (pMAL630), shows lower GFP expression (strain EMAL230) in blue light than OptoLAC1 or OptoLAC2 (Fig. 1b). However, inserting a *lacO* sequence also weakens P_{FixK2}, which lowers cI-mediated repression of *lacI* in the dark (Extended Data Fig. 1c), and maximal GFP expression by OptoLAC3. Quantitative western blot analysis confirmed that the positive feedback loop in OptoLAC3 increases the expression of LacI in the light by as much as 60.7- and 53.1-fold relative to OptoLAC1 and OptoLAC2, respectively (Extended Data Fig. 2). Unlike OptoLAC1 and OptoLAC2, LacI levels in OptoLAC3 remain detectable even after 8 h in the dark (yet 66 times lower than in the light), explaining the lower maximal expression achieved with OptoLAC3. Nevertheless, OptoLAC3 achieves a 60.9-fold induction of gene expression in the dark, which is the highest of the OptoLAC circuits, and still twice the expression achieved from P_{BBA} (Fig. 1b). All three OptoLAC circuits remain IPTG-inducible (Extended Data Fig. 3), and OptoLAC1 and OptoLAC2 are functional at 37 °C (Fig. 1b) as well as 18 °C (Extended Data Fig. 4). OptoLAC1, 2 and 3 represent the first suite of optogenetic circuits that harness the *lac* operon to control gene expression in *E. coli* with light.

Characterization of OptoLAC circuits. To test the tunability of the OptoLAC circuits, we grew strains containing OptoLAC1 (EMAL68) or OptoLAC3 (EMAL230) under different duty cycles of light. With 1% of light exposure (10 s of light per 1,000 s), OptoLAC1 achieves 61% of maximal expression, and only 10% of light is enough to reach 99% of maximum repression (Fig. 2a). OptoLAC3 is even more sensitive than OptoLAC1, achieving full repression under only 1% of light duty cycle (Fig. 2a). Although both circuits should, in principle, be controllable by the intensity of continuous illumination, their high sensitivity to even the lowest intensities we can practically provide (5 μmol m^{-2} s^{-1}, Extended Data Fig. 5) makes them more easily tunable using light duty cycles. The differences in light sensitivities between circuits may be useful for different applications: for example, OptoLAC1 is best suited to maintain intermediate levels of expression, while OptoLAC3 can better achieve full gene repression when light penetration is limited.

To test whether OptoLAC circuits can control other *lacO*-containing promoters besides the $P_{T5\text{-}lacO}$ promoter, we used OptoLAC1 to control GFP expression from P_{lacUV5}[15] and P_{trc}[16] with light. Both promoters show light-tunable repression with varying degrees of maximal gene expression in the dark according to the core promoter strength (Fig. 2b). This finding demonstrates that our OptoLAC circuits can be used to control different IPTG-inducible promoters, which facilitates the retrofitting of many existing systems with light controls.

Inducible promoters are frequently used for dynamic control in metabolic engineering to produce fuels and chemicals from renewable sources, such as glucose or xylose. In addition, different applications require minimal or rich media such as LB medium or super optimal broth (SOB) medium. We therefore tested OptoLAC1 in M9 minimal salts medium with glucose or xylose, as well as in LB or SOB media, and found it to be effective at controlling gene expression with light in all media tested (Fig. 2c). However, OptoLAC1 is more light-sensitive in rich media than in minimal media (Supplementary Note 3), while its maximal gene expression in the dark is greater in glucose than in xylose. OptoLAC circuits can control gene expression not only temporally in liquid media, but also spatially in solid media by shielding specific sections of an LB agar plate from blue light (Extended Data Fig. 6). Therefore, OptoLAC circuits provide spatiotemporal control over gene expression in different media for the potential benefit of many applications.

We next compared OptoLAC circuits with IPTG, the current gold standard method to induce gene expression in *E. coli*. We performed two-phase time-course experiments to compare these systems, implementing a growth phase (light/no IPTG) followed by a production phase (darkness/IPTG) (Methods). Expression of GFP from OptoLAC circuits is detectable 2–4 h after inducing with darkness, whereas IPTG induction responds more rapidly with stronger GFP expression by the second hour after induction (Fig. 2d). This is consistent with LacI degradation, required to activate gene expression in OptoLAC circuits, being inherently slower than allosteric inhibition of LacI by IPTG. However, it still takes 10 h to reach full induction of GFP with IPTG, at which point the levels of expression achieved with OptoLAC1 and OptoLAC2 are higher by 63% and 41%, respectively. GFP expression obtained with IPTG induction is matched by OptoLAC1 and OptoLAC2 ~4–5 h after induction, and by OptoLAC3 after 8 h. Importantly, exposing the cultures containing OptoLAC circuits to blue light for the entire time course keeps GFP expression repressed (Fig. 2e). Moreover, while strains containing OptoLAC circuits have a slightly increased lag phase compared to the IPTG-induced control, they show comparable growth rates in exponential phase and final biomass yields (Extended Data Fig. 7). Despite their initial delay in induction, OptoLAC circuits eventually catch up and even exceed the induction levels achieved with IPTG, with minimal impact on cell growth, suggesting that the inhibition of LacI by IPTG is incomplete and its transcriptional repression is ultimately more effective.

A major advantage of optogenetic controls over chemical induction is reversibility, as turning lights on and off is easier and faster than changing media. To explore this capability, we tested the on-to-off kinetics of OptoLAC circuits using an unstable $P_{T5\text{-}lacO}$-GFP reporter fused to a C-terminal SsrA (AAV) tag (pMAL897) and inducing cultures in the dark for 3 h before turning on the lights for 6 h (Methods). OptoLAC1 (EMAL343) exhibits a 1.5-h delay before GFP levels decrease, with an ~1-h half-life signal decay thereafter (Fig. 2f). The timescale of these experiments does not permit sufficient GFP-SsrA (AAV) expression with the weaker OptoLAC2 and OptoLAC3 to carry out

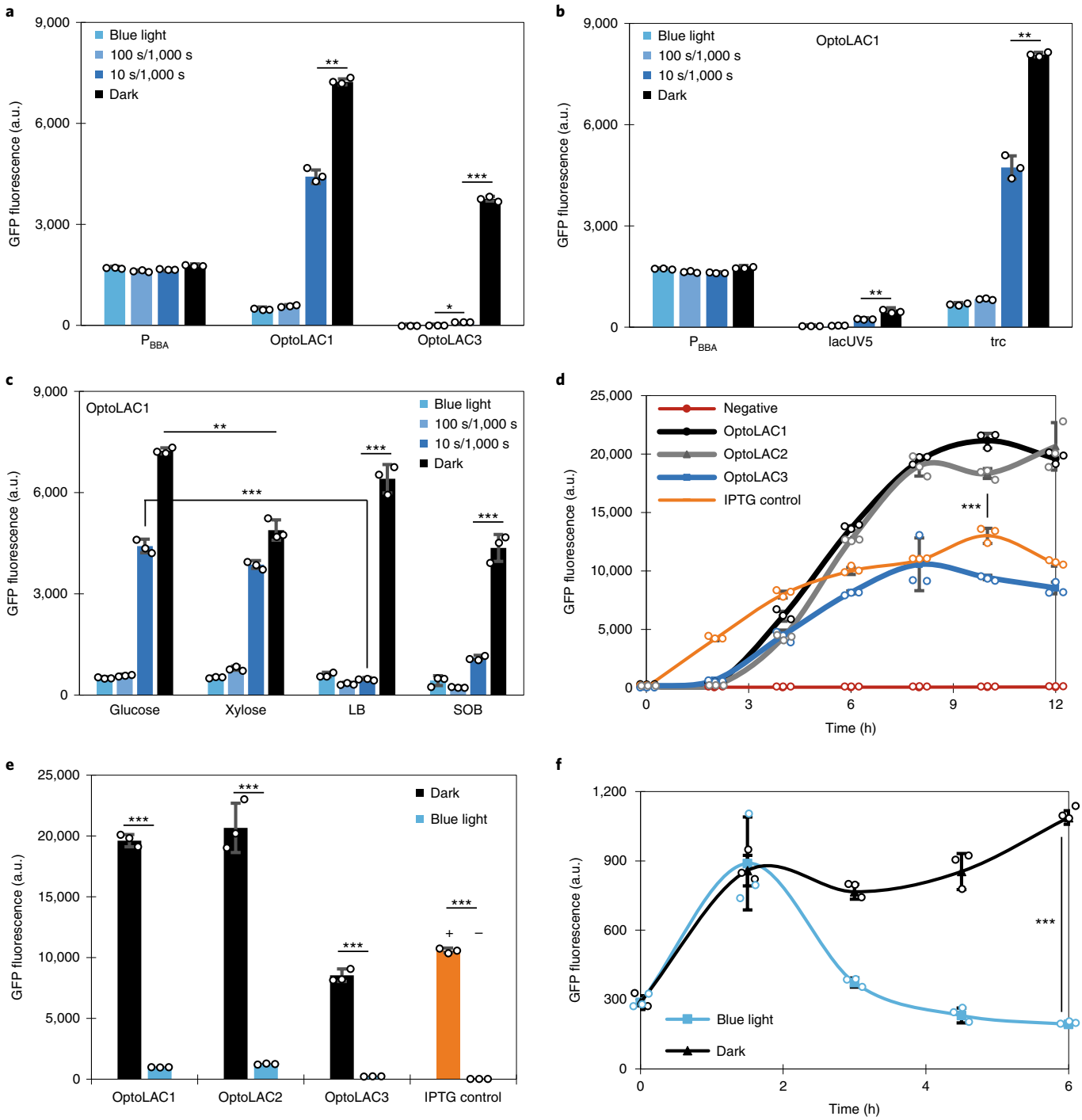

Fig. 2 | OptoLAC circuit characterization. a, GFP expression from P_{BBA} (EMAL231) or from $P_{T5\text{-}lacO}$ controlled by OptoLAC1 (EMAL68) or OptoLAC3 (EMAL230), under full light, 100 s on/1,000 s, 10 s on/1,000 s and full darkness. From left to right: $P = 0.0017$, $P = 0.0108$, $P < 0.00001$. **b**, GFP expression from P_{BBA} (EMAL231) or controlled by OptoLAC1 from P_{lacUV5} (EMAL267) or P_{trc} (EMAL268). From left to right: $P = 0.0011$, $P = 0.00349$. **c**, GFP expression from $P_{T5\text{-}lacO}$ controlled by OptoLAC1 (EMAL68) in M9 medium + 2% glucose, M9 + 2% xylose, LB medium and SOB medium. From left to right: $P = 0.00552$, $P = 0.000025$, $P = 0.000011$, $P = 0.000136$. **d**, Time course of GFP expression from $P_{T5\text{-}lacO}$ controlled by OptoLAC1 (EMAL68; black circles), OptoLAC2 (EMAL69; gray triangles), OptoLAC3 (EMAL230; blue squares) or IPTG (EMAL77; orange dashes) compared to a negative control lacking GFP (EMAL229; red circles). $P = 0.000154$. **e**, GFP expression from **d** at 12 h, including uninduced controls where cultures were kept in blue light or without IPTG. From left to right: $P < 0.00001$, $P < 0.00001$, $P < 0.00001$, $P < 0.00001$. **f**, Time course of destabilized GFP expression from $P_{T5\text{-}lacO}$ controlled by OptoLAC1 (EMAL343) in blue light (blue squares) or darkness (black triangles). $P = 0.000015$. $^{*}P < 0.05$, $^{**}P < 0.01$, $^{***}P < 0.001$. Statistics are derived using a two-sided *t*-test. All data are shown as median values of 10,000 single-cell flow cytometry events; error bars represent 1 s.d. of $n = 3$ biologically independent samples; open circles represent individual data points. Data are representative of $n = 3$ independent experiments.

the same measurements, although the observed trends are as expected (Supplementary Fig. 1a,b and Supplementary Note 4). Although OptoLAC circuits are specifically designed for efficient gene induction in the dark, at least OptoLAC1 offers reversibility in short fermentations (9 h), which cannot be replicated with IPTG induction.

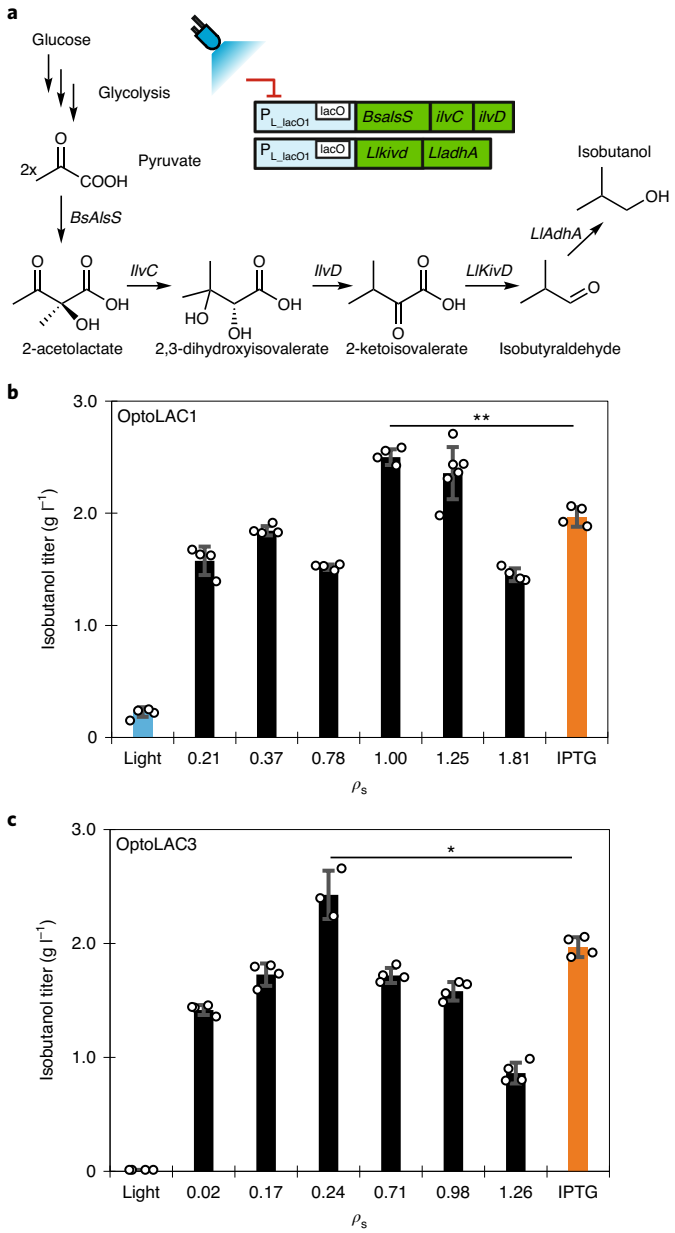

Fig. 3 | Dynamic control of isobutanol production using OptoLAC circuits. a, Optogenetic control of the isobutanol biosynthetic pathway, composed of *BsalsS*, *ilvC*, *ilvD*, *LlKivd* and *LladhA*, expressed from $P_{L\text{-}LacO1}$. **b**,**c**, Isobutanol production controlled with OptoLAC1 (EMAL199) (**b**) or OptoLAC3 (EMAL239) (**c**) when switching cultures from blue light to darkness at different cell densities (ρ_s values, black) or uninduced (blue), as well as induced with IPTG (EMAL201) at optimal cell density (orange). For **b**, $P = 0.00116$; from left to right, $n = 4, 4, 4, 4, 4, 6, 4, 4$. For **c**, $P = 0.0116$; biological replicates from left to right, $n = 4, 4, 4, 3, 4, 4, 4, 4$. $^*P < 0.05$, $^{**}P < 0.01$. Statistics are derived using a two-sided *t*-test. All data are shown as mean values; error bars represent the s.d. of biologically independent samples; open circles represent individual data points. Data are representative of $n = 2$ independent experiments.

Optogenetic control of isobutanol production. Given the potential of optogenetics for metabolic engineering[4,5,17], we tested OptoLAC circuits in light-controlled fermentations for chemical production. First, we applied them to control the biosynthesis of the advanced biofuel isobutanol (Fig. 3a)[18]. We adapted previously developed plasmids containing an IPTG-inducible isobutanol pathway[19,20] to our optogenetic platform (Methods). This generated strains that control isobutanol production using OptoLAC1 (EMAL199), OptoLAC2 (EMAL200), OptoLAC3 (EMAL239) or IPTG (EMAL201). The optical density at 600 nm (OD_{600}) at which we switch fermentations controlled with OptoLAC circuits from light to darkness (ρ_s) has a substantial impact on final isobutanol titers (Methods). Those induced at their optimal ρ_s values achieve as much as 27% higher isobutanol titers ($2.5 \pm 0.1\,g\,l^{-1}$ and $2.4 \pm 0.2\,g\,l^{-1}$ with OptoLAC1 and OptoLAC3, respectively) than fermentations induced with IPTG at their optimal OD_{600} of induction ($2.0 \pm 0.1\,g\,l^{-1}$, $OD_{600} = 1.4$) (Fig. 3b,c and Extended Data Fig. 8a). The optimal ρ_s values differ substantially between OptoLAC1 ($\rho_s = 1.0$) and OptoLAC3 ($\rho_s = 0.24$), probably due to differences in circuit strength (Supplementary Note 5). Thus, OptoLAC circuits can replace IPTG with darkness as an inducing agent in *E. coli* fermentations for chemical production.

Optogenetic control of mevalonate production. To test whether our optogenetic circuits can be applied to other metabolic pathways, we used them to produce mevalonate, an important terpenoid precursor. Again, we adapted a previously described IPTG-inducible plasmid[18] containing the mevalonate pathway (Fig. 4a). We constructed strains in which mevalonate biosynthesis is controlled with light using OptoLAC1 (EMAL208), OptoLAC2 (EMAL209) or OptoLAC3 (EMAL235), as well as an IPTG-induced control (EMAL135). OptoLAC1 and OptoLAC2 achieve the highest titers of $6.4 \pm 0.2\,g\,l^{-1}$ and $6.1 \pm 0.2\,g\,l^{-1}$, respectively, at similar ρ_s values ($\rho_s = 0.17$–0.23), which exceed the titer obtained with IPTG at its optimal OD_{600} of induction ($5.2 \pm 0.1\,g\,l^{-1}$, $OD_{600} = 0.06$) by as much as 24% (Fig. 4b,c and Extended Data Fig. 8b). The low optimal ρ_s values and high performance of OptoLAC1 and OptoLAC2 suggest that early and high maximal induction are key to optimizing mevalonate production (Supplementary Note 5). OptoLAC circuits can thus control different metabolic pathways with light, improving upon the titers obtained with IPTG induction.

To test the scalability of our approach, we used EMAL208 (OptoLAC1) to produce mevalonate in a light-controlled 2-l bioreactor. In addition to temperature, pH and dissolved oxygen controls, we installed blue light panels to illuminate ~76% of the fermentation bulk surface (Supplementary Fig. 2) until the culture reached the optimal ρ_s ($OD_{600} = 0.17$). For the first 3 h after induction, mevalonate production is undetectable, demonstrating that blue light effectively represses the mevalonate pathway during the growth phase (Fig. 4d). By the sixth hour after induction, mevalonate production increases rapidly, reaching $6.3 \pm 0.2\,g\,l^{-1}$ after 72 h of induction. Overall, our results suggest that OptoLAC circuits respond equally to the light penetration achievable in fermentations scaled up at least three orders of magnitude (Supplementary Note 6).

Optogenetic control of recombinant protein production. To demonstrate the ability of OptoLAC circuits to control LacI-regulated (IPTG-inducible) promoters in other applications, we tested them for light control of recombinant protein production. We adapted our platform to the workhorse B-strain for protein production, BL21 DE3, by deleting its two endogenous copies of *lacI*, resulting in EMAL255 (hereafter OptoBL). We also removed the constitutive copy of *lacI* from pCri-8b (containing P_{T7}-YFP (yellow fluorescent protein)[21]) to produce plasmid pC85. Finally, we reconstructed OptoLAC1 and OptoLAC2 into a pACYC-derived[22] backbone, resulting in OptoLAC1B (pMAL658) and OptoLAC2B (pMAL659), respectively, which have different origins of replication and are thus compatible with commonly used pET and pCri protein production vectors (Supplementary Table 1).

Using these tools, we created EMAL284 (Supplementary Table 2), which can be induced with darkness using OptoLAC1B to produce YFP (Methods). OptoLAC1B keeps YFP tightly repressed

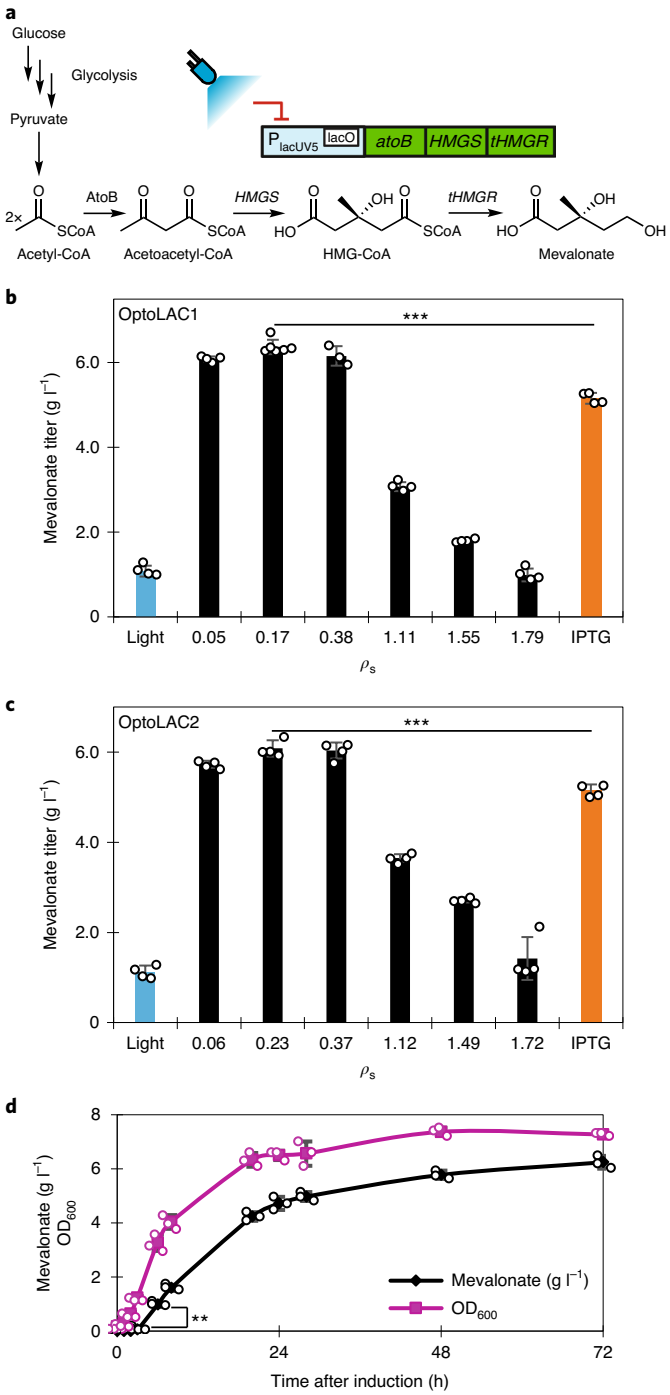

Fig. 4 | Dynamic control of mevalonate production using OptoLAC circuits and scale-up. a, The mevalonate biosynthetic pathway, composed of *atoB*, *HGMS* and *tHMGR*, expressed from P_{lacUV5}. **b**,**c**, Mevalonate production controlled with OptoLAC1 (EMAL208) (**b**) or OptoLAC2 (EMAL209) (**c**) when switching cultures from blue light to darkness at different cell densities (ρ_s values, black) or uninduced (blue), as well as induced with IPTG (EMAL135) (orange). For **b**, $P = 0.000314$; biological replicates from left to right, $n = 4, 4, 6, 3, 4, 4, 4, 4$. For **c**, $P = 0.000689$; four biological replicates ($n = 4$) for all conditions. **d**, Light-controlled mevalonate production in a 2-l bioreactor; $P = 0.00213$. $^{**}P < 0.01$, $^{***}P < 0.001$. Statistics are derived using a two-sided *t*-test. All data are shown as mean values; error bars represent the s.d. of biologically independent samples for **b** and **c**, or three independent bioreactor runs for **d**; open circles represent individual data points. Data for **b** and **c** are representative of $n = 2$ independent experiments.

under light ($t = 0$ h in Fig. 5a) and effectively induces its production in the dark. Although OptoLAC1B shows an ~2-h delay in detectable protein production, after 9–12 h of darkness induction, the levels of protein production achieved by OptoLAC1B are comparable to those achieved with an IPTG-induced control (EMAL283; Fig. 5a). The optimal cell density of induction for YFP production (after 9 h) is similar for both IPTG and darkness ($OD_{600} = 0.1$, Extended Data Fig. 9a). Similar to OptoLAC circuits in OptoMG, OptoLAC1B has a minimal impact on OptoBL growth in two-phase fermentations, causing a slight decrease in growth rate compared to the IPTG-induced control, but no significant difference in final biomass yield (Extended Data Fig. 10a). Under non-inducing conditions (light/no IPTG), the impact of OptoLAC1B is smaller than that caused by plasmid pRARE2 in the Rosetta 2 strain (Extended Data Fig. 10b). OptoLAC circuits can thus be robustly transferred across different strains and plasmids for different biotechnological applications.

As a second example for recombinant protein production, we chose FdeR, a transcription factor from *Herbaspirillum seropedicae*[23]. We transformed OptoBL with OptoLAC1B (pMAL658) or OptoLAC2B (pMAL659), and pMAL887 to produce EMAL335 and EMAL336, respectively (Supplementary Tables 1 and 2). OptoLAC2B displays tighter control over FdeR expression when cells are grown in constant blue light for 12 h (Extended Data Fig. 9b). Similar to YFP with OptoLAC1B, FdeR production from OptoLAC2B is tightly controlled before induction ($t = 0$ h in Fig. 5b) and, despite an ~2-h delay, FdeR production with OptoLAC2B is comparable to that of an IPTG-inducible control (EMAL329) 9–12 h after induction (Fig. 5b). Moreover, FdeR production remains high over a broader range of ρ_s values ($OD_{600} = 0.2$–1.0) compared to cell densities of IPTG induction of EMAL329 ($OD_{600} = 0.5$–1.0) (Extended Data Fig. 9c). Thus, both OptoLAC1B and OptoLAC2B can control the production of different recombinant proteins at yields comparable to those achieved with IPTG induction.

Easy tunability of gene expression is a potential advantage of optogenetic control over chemical induction. To showcase this capability, we quantified YFP and FdeR production induced with different duty cycles of blue light (EMAL284, EMAL336) or different IPTG concentrations (EMAL283, EMAL329). Both EMAL283 and EMAL329 show optimal YFP or FdeR production at intermediate concentrations of IPTG (500 µM and 100 µM, respectively), with higher concentrations leading to reduced protein levels (Fig. 5c and Extended Data Fig. 9d). By contrast, EMAL284 and EMAL336, containing OptoLAC1B and OptoLAC2B, respectively, show maximum production in full darkness with a monotonic light response, which facilitates tunability (Fig. 5c and Extended Data Fig. 9d). OptoLAC1B and OptoLAC2B can be induced with IPTG even when cells are kept in blue light (Supplementary Fig. 3), but this significantly hampers cell growth (Extended Data Fig. 10b), probably due to the burden imposed by the strong T7 polymerase when inhibiting an already destabilized LacI. Our findings illustrate the potential of optogenetics to tune the quantity and rate of protein production with light, which may impact the proper folding and solubility of recombinant proteins.

Discussion

OptoLAC circuits offer powerful capabilities to control gene expression in *E. coli* with light. Although optogenetic tools have previously been developed for this organism[8–10], including for protein production[24–26], our approach harnesses the *lac* operon, allowing the direct substitution of IPTG with darkness as an inducing agent. This replacement is feasible in at least two common applications: metabolic engineering and recombinant protein production. All IPTG-inducible vectors we tested, which use five different *lacO*-containing promoters ($P_{T5\text{-}lacO}$, P_{lacUV5}, P_{trc}, P_{L_lacO1} and P_{T7}), could be adapted to work with OptoLAC circuits and Δ*lacI* strains

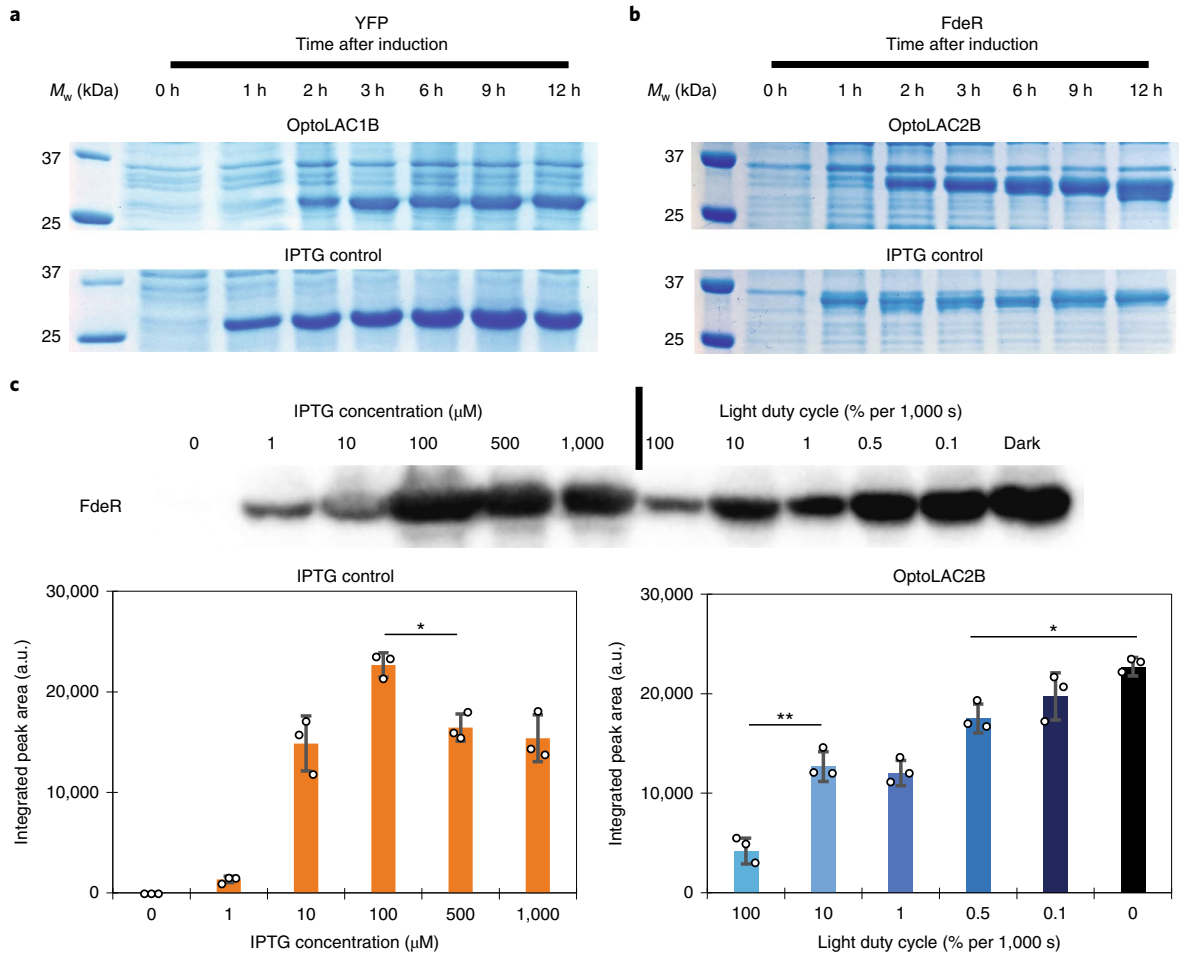

Fig. 5 | Light-controlled recombinant protein production in *E. coli* B strain (OptoBL). a, Time course of YFP production, induced by switching cultures from blue light to darkness using OptoLAC1B (EMAL284, top) or adding IPTG (EMAL283, bottom). **b**, Time course of FdeR production, induced by switching cultures from blue light to darkness using OptoLAC2B (EMAL336, top) or adding IPTG (EMAL329, bottom). **c**, Tunability of FdeR production using different doses of light or concentrations of IPTG, resolved and quantified via western blot. Left panel: $P = 0.0153$. Right panel, from left to right: $P = 0.00776$, $P = 0.0254$. Loading controls and uncropped gels and blots, including those used for quantification in **c** (samples derived from the same experiment and processed in parallel) are provided as source data. $^*P < 0.05$, $^{**}P < 0.01$. Statistics are derived using a two-sided *t*-test. All data are shown as mean values; error bars represent the standard deviation of $n = 3$ biologically independent samples; open circles represent individual data points. Data are representative of $n = 2$ independent experiments.

(OptoMG or OptoBL) for optogenetic control. This only involves removing any *lacI* copy and ensuring that each plasmid uses a unique selection marker and origin of replication.

Optogenetics may help balance the levels of expression of different metabolic enzymes, which greatly impacts the performance of engineered pathways[27]. This key challenge in metabolic engineering is currently addressed by assembling large numbers of constructs, usually in biofoundries[28], to combinatorially test different enzyme expression levels[29,30]. However, the ability of OptoLAC circuits to finely tune gene expression from different promoters could transform this practice by testing varying pulses of light instead of copious numbers of constitutive constructs. The testable expression space of our OptoLAC circuits could be further expanded using mutations that sensitize or invert the light response of the YF1 protein[31,32]. Furthermore, OptoLAC circuits could be combined with other circuits that respond orthogonally to different wavelengths of light (for example, green[9], red or infrared[8]) to enable multivariate modular metabolic engineering to balance pathways[33]. Such a polychromatic approach would not only dramatically reduce the number of constructs required to balance complex metabolic pathways, but also increase the resolution at which levels of enzyme expression could be screened for pathway optimization.

Although we have shown optogenetics can enable light-controlled fermentations in lab-scale bioreactors, potential challenges to light penetration raise concerns about its applicability in larger industrial-scale bioreactors, extrapolated in part from previous experience with algae bioprocesses. However, light penetration is unlikely to be as limiting to our systems as it is for photosynthetic organisms. In cell cultures of algae or cyanobacteria, there is a stoichiometric relationship between the photons absorbed by the photosynthetic systems and adenosine triphosphate output[34]. The light-harvesting antennas in photosynthetic organisms present an additional challenge to effectively illuminate cultures for robust cell growth and production[35]. In contrast, our optogenetic circuits are not required for energy metabolism and *E. coli* has not evolved to compete for light harvesting. Instead, our circuits control cI expression, which we hypothesize leads to accumulation of LacI mRNA and protein[36,37] under blue light that does not immediately subside when cells are switched to darkness. In this sense, our optogenetic circuits have an inherent 'memory' of having been exposed to blue light, which makes the requirements for light penetration more lenient.

This memory is evident in kinetics experiments (Fig. 2d), bioreactor fermentations (Fig. 4d) and protein production (Fig. 5a,b). In

all these instances, the response of our circuits has an ~2-h delay, as opposed to the almost immediate response to IPTG as an allosteric LacI inhibitor. In addition to alleviating demanding light penetration conditions, this feature of OptoLAC circuits may also be useful to mimic slow-acting inducible systems, such as those based on quorum sensing, which have been effectively used as auto-inducible systems for chemical production[38]. A gradual decrease of illumination could be used to mirror the gradual increase of quorum-sensing molecule concentrations, but with the advantage that the onset and rate of light dimming can be easily controlled and operated reversibly using our OptoLAC circuits. Autoinduction strategies may also be possible in which genes are gradually expressed as increasing optical densities reduce light penetration in large bioreactors.

In addition to being effective for metabolic engineering in K-12 strains, OptoLAC circuits are also applicable for recombinant protein production in B-strains. Light controls may be particularly useful for recombinant proteins that are difficult to produce. For example, proteins toxic to *E. coli* are often produced at very low yields or require the addition of inhibitors against their toxic activity[39]. Additionally, rates of protein expression can be too high to keep recombinant proteins from aggregating or forming inclusion bodies. This problem can sometimes be alleviated by inducing at low temperatures[40] and/or using autoinduction media[41]. However, the fine tunability of gene expression afforded by light could potentially enhance the yields of toxic proteins by tempering their expression levels, or improve the quality and solubility of proteins that are difficult to produce by better regulating their rates of expression.

OptoLAC circuits open the door to replacing IPTG with light for a broad number of applications. In industrial fermentations, eliminating IPTG (or other chemical inducers) would reduce costs. Additionally, it would enable dynamic controls in processes for which the use of chemical inducers is prohibitively expensive. Beyond chemical and recombinant protein production, IPTG induction has been used for a variety of research applications, including persistence[42], bacterial motility[43], inducible protein degradation[44] and biofilm formation[45]. Furthermore, the LacI repressor has been exported to other bacteria for IPTG inducibility[46–48]. Therefore, OptoLAC circuits may be applicable in a wide range of systems originally designed to be IPTG-inducible, providing them with the enhanced capabilities typically afforded by light, such as fine tunability, reversibility and spatiotemporal control.

Online content

Any methods, additional references, Nature Research reporting summaries, source data, extended data, supplementary information, acknowledgements, peer review information; details of author contributions and competing interests; and statements of data and code availability are available at https://doi.org/10.1038/s41589-020-0639-1.

Received: 16 November 2019; Accepted: 31 July 2020;
Published online: 7 September 2020

References

1. Pontrelli, S. et al. *Escherichia coli* as a host for metabolic engineering. *Metab. Eng.* **50**, 16–46 (2018).
2. Sanford, K., Chotani, G., Danielson, N. & Zahn, J. A. Scaling up of renewable chemicals. *Curr. Opin. Biotechnol.* **38**, 112–122 (2016).
3. Burgard, A., Burk, M. J., Osterhout, R., Van Dien, S. & Yim, H. Development of a commercial scale process for production of 1,4-butanediol from sugar. *Curr. Opin. Biotechnol.* **42**, 118–125 (2016).
4. Lalwani, M. A., Zhao, E. M. & Avalos, J. L. Current and future modalities of dynamic control in metabolic engineering. *Curr. Opin. Biotechnol.* **52**, 56–65 (2018).
5. Zhao, E. M. et al. Optogenetic regulation of engineered cellular metabolism for microbial chemical production. *Nature* **555**, 683–687 (2018).
6. Jacob, F. & Monod, J. Genetic regulatory mechanisms in the synthesis of proteins. *J. Mol. Biol.* **3**, 318–356 (1961).
7. Donovan, R. S., Robinson, C. W. & Click, B. R. Review: optimizing inducer and culture conditions for expression of foreign proteins under the control of the lac promoter. *J. Ind. Microbiol.* **16**, 145–154 (1996).
8. Levskaya, A. Engineering *Escherichia coli* to see light. *Nature* **438**, 441–442 (2005).
9. Tabor, J. J., Levskaya, A. & Voigt, C. A. Multichromatic control of gene expression in *Escherichia coli*. *J. Mol. Biol.* **405**, 315–324 (2011).
10. Ohlendorf, R., Vidavski, R. R., Eldar, A., Moffat, K. & Möglich, A. From dusk till dawn: one-plasmid systems for light-regulated gene expression. *J. Mol. Biol.* **416**, 534–542 (2012).
11. Möglich, A. et al. Design and signaling mechanism of light-regulated histidine kinases. *J. Mol. Biol.* **385**, 1433–1444 (2009).
12. Orman, M. A. & Brynildsen, M. P. Dormancy is not necessary or sufficient for bacterial persistence. *Antimicrob. Agents Chemother.* **57**, 3230–3239 (2013).
13. Tu, G.-F., Reid, G. E., Zhang, J.-G., Moritz, R. L. & Simpson, R. J. C-terminal extension of truncated recombinant proteins in *Escherichia coli* with a 10Sa RNA decapeptide. *J. Biol. Chem.* **270**, 9322–9326 (1995).
14. Hentschel, E. et al. Destabilized eYFP variants for dynamic gene expression studies in *Corynebacterium glutamicum*. *Microb. Biotechnol.* **6**, 196–201 (2013).
15. Studier, F. W. & Moffatt, B. A. Use of bacteriophage T7 RNA polymerase to direct selective high-level expression of cloned genes. *J. Mol. Biol.* **189**, 113–130 (1986).
16. Brosius, J., Erfle, M. & Storella, J. Spacing of the -10 and -35 regions in the tac promoter. Effect on its in vivo activity. *J. Biol. Chem.* **260**, 3539–3541 (1985).
17. Zhao, E. M. et al. Light-based control of metabolic flux through assembly of synthetic organelles. *Nat. Chem. Biol.* **15**, 589–597 (2019).
18. Martin, V. J. J., Pitera, D. J., Withers, S. T., Newman, J. D. & Keasling, J. D. Engineering a mevalonate pathway in *Escherichia coli* for production of terpenoids. *Nat. Biotechnol.* **21**, 796–802 (2003).
19. Atsumi, S., Hanai, T. & Liao, J. C. Non-fermentative pathways for synthesis of branched-chain higher alcohols as biofuels. *Nature* **451**, 86–89 (2008).
20. Baez, A., Cho, K. M. & Liao, J. C. High-flux isobutanol production using engineered *Escherichia coli*: a bioreactor study with in situ product removal. *Appl. Microbiol. Biotechnol.* **90**, 1681–1690 (2011).
21. Goulas, T. et al. The pCri system: a vector collection for recombinant protein expression and purification. *PLoS ONE* **9**, e112643 (2014).
22. Chang, A. C. Y. & Cohen, S. N. Construction and characterization of amplifiable multicopy DNA cloning vehicles derived from the P15A cryptic miniplasmid. *J. Bacteriol.* **134**, 1141–1156 (1978).
23. Marin, A. M. et al. Naringenin degradation by the endophytic diazotroph *Herbaspirillum seropedicae* SmR1. *Microbiology* **159**, 167–175 (2013).
24. Baumschlager, A., Aoki, S. K. & Khammash, M. Dynamic blue light-inducible T7 RNA polymerases (Opto-T7RNAPs) for precise spatiotemporal gene expression control. *ACS Synth. Biol.* **6**, 2157–2167 (2017).
25. Chou, C., Young, D. D. & Deiters, A. Photocaged T7 RNA polymerase for the light activation of transcription and gene function in pro- and eukaryotic cells. *ChemBioChem* **11**, 972–977 (2010).
26. Binder, D. et al. Light-responsive control of bacterial gene expression: precise triggering of the lac promoter activity using photocaged IPTG. *Integr. Biol.* **6**, 755–765 (2014).
27. Wu, G. et al. Metabolic burden: cornerstones in synthetic biology and metabolic engineering applications. *Trends Biotechnol.* **34**, 652–664 (2016).
28. Hillson, N. et al. Building a global alliance of biofoundries. *Nat. Commun.* **10**, 1038–1041 (2019).
29. Awan, A. R. et al. Biosynthesis of the antibiotic nonribosomal peptide penicillin in baker's yeast. *Nat. Commun.* **8**, 15202 (2017).
30. Latimer, L. N. & Dueber, J. E. Iterative optimization of xylose catabolism in *Saccharomyces cerevisiae* using combinatorial expression tuning. *Biotechnol. Bioeng.* **114**, 1301–1309 (2017).
31. Hennemann, J. et al. Optogenetic control by pulsed illumination. *ChemBioChem* **19**, 1296–1304 (2018).
32. Diensthuber, R. P., Bommer, M., Gleichmann, T. & Möglich, A. Full-length structure of a sensor histidine kinase pinpoints coaxial coiled coils as signal transducers and modulators. *Structure* **21**, 1127–1136 (2013).
33. Ajikumar, P. K. et al. Isoprenoid pathway optimization for taxol precursor overproduction in *Escherichia coli*. *Science* **330**, 70–74 (2010).
34. Melis, A. et al. Chromatic regulation in *Chlamydomonas reinhardtii* alters photosystem stoichiometry and improves the quantum efficiency of photosynthesis. *Photosynth. Res.* **47**, 253–265 (1996).
35. Ort, D. R., Zhu, X. & Melis, A. Optimizing antenna size to maximize photosynthetic efficiency. *Plant Physiol.* **155**, 79–85 (2011).
36. Nilsson, G., Belasco, J. G., Cohen, S. N. & Von Gabain, A. Growth-rate dependent regulation of mRNA stability in *Escherichia coli*. *Nature* **312**, 75–77 (1984).
37. Gottesman, S. Proteases and their targets in *Escherichia coli*. *Annu. Rev. Genet.* **30**, 465–506 (1996).

38. Doong, S. J., Gupta, A. & Prather, K. L. J. Layered dynamic regulation for improving metabolic pathway productivity in *Escherichia coli*. *Proc. Natl Acad. Sci. USA* **115**, 2964–2969 (2018).
39. Valiyaveetil, F. I., MacKinnon, R. & Muir, T. W. Semisynthesis and folding of the potassium channel KcsA. *J. Am. Chem. Soc.* **124**, 9113–9120 (2002).
40. San-Miguel, T., Pérez-Bermúdez, P. & Gavidia, I. Production of soluble eukaryotic recombinant proteins in *E. coli* is favoured in early log-phase cultures induced at low temperature. *Springerplus* **2**, 1–4 (2013).
41. Studier, F. W. Protein production by auto-induction in high density shaking cultures. *Protein Expr. Purif.* **41**, 207–234 (2005).
42. Mok, W. W. K. & Brynildsen, M. P. Timing of DNA damage responses impacts persistence to fluoroquinolones. *Proc. Natl Acad. Sci. USA* **115**, E6301–E6309 (2018).
43. Partridge, J. D., Nhu, N. T. Q., Dufour, Y. S. & Harshey, R. M. *Escherichia coli* remodels the chemotaxis pathway for swarming. *mBio* **10**, 1–16 (2019).
44. McGinness, K. E., Baker, T. A. & Sauer, R. T. Engineering controllable protein degradation. *Mol. Cell* **22**, 701–707 (2006).
45. Zuo, R., Hashimoto, Y., Yang, L., Bentley, W. E. & Wood, T. K. Autoinducer 2 controls biofilm formation in *Escherichia coli* through a novel motility quorum-sensing regulator (MqsR, B3022). *J. Bacteriol.* **188**, 305–316 (2006).
46. Ronchel, M. C. et al. Characterization of cell lysis in *Pseudomonas putida* induced upon expression of heterologous killing genes. *Appl. Environ. Microbiol.* **64**, 4904–4911 (1998).
47. Rittmann, D., Lindner, S. N. & Wendisch, V. F. Engineering of a glycerol utilization pathway for amino acid production by *Corynebacterium glutamicum*. *Appl. Environ. Microbiol.* **74**, 6216–6222 (2008).
48. Nguyen, H. D., Phan, T. T. P. & Schumann, W. Expression vectors for the rapid purification of recombinant proteins in *Bacillus subtilis*. *Curr. Microbiol.* **55**, 89–93 (2007).

Methods

Plasmid construction. Plasmids were cloned into *E. coli* strain DH5α made chemically competent using the Inoue method[49]. Transformants were inoculated on LB agar plates at 37 °C with appropriate antibiotics: 100 μg ml^{-1} ampicillin, 100 μg ml^{-1} carbenicillin, 50 μg ml^{-1} kanamycin, 34 μg ml^{-1} chloramphenicol or 50 μg ml^{-1} spectinomycin. Epoch Life Science Miniprep, Omega Gel Extraction and Omega PCR purification kits were used to extract and purify plasmids and DNA fragments. Backbones and inserts were either digested using restriction enzymes purchased from NEB or PCR-amplified using Q5 polymerase from NEB or CloneAmp HiFi PCR premix from Takara Bio. One-step Gibson isothermal assembly reactions were performed based on previously described protocols[50]. Primers were ordered from Integrated DNA Technologies or Genewiz. All plasmids were verified using Sanger sequencing from Genewiz. We avoided using tandem repeats to prevent recombination after transformation and thus did not observe instability of strains or plasmids.

Promoters, operators and tags (P_{BBa_J23100}, P_{lacUV5}, P_{trc}, *lacO*, *ssrA* tags) were inserted by Gibson assembly, using extended-length primers with homology arms. Plasmids pDusk and pDawn were obtained as a gift from A. Möglich (Addgene 43795 and 43796, respectively)[10]. Plasmid pMevT, used for mevalonate production, was obtained as a gift from J. Keasling (Addgene 17815)[18]. Plasmids pSA65 and pSA69, used for isobutanol production, were obtained as gifts from J. Liao[19,51]. A detailed description of all the plasmids used in this study is provided in Supplementary Table 1.

Bacterial cell culture growth and measurements. Single colonies from LB+ antibiotic agar plates were inoculated into liquid media and grown in 96-well (USA Scientific Item CC7672-7596) or 24-well (USA Scientific Item CC7672-7524) plates. Strains were grown in a New Brunswick Innova 4000 or Scientific Industries Genie Temp-Shaker 300 (SI-G1600) incubator shaker set to 37 °C and shaken at 200 r.p.m. (19-mm orbital diameter). K strains were cultured in M9 minimal salts medium supplemented with 0.2% wt/vol casamino acids (Bio Basic), K3 trace metal mixture[52], 2% wt/vol (20 g l^{-1}) glucose, and appropriate antibiotics (using the previously specified concentrations), unless stated otherwise. B strains were cultured in LB medium (Miller) supplemented with appropriate antibiotics (using the previously specified concentrations). Light-sensitive strains were grown under blue light to keep expression of proteins or metabolic pathways repressed. To stimulate cells with blue (465 nm) light, we used LED panels (HQRP New Square 12-inch Grow Light Blue LED 14 W) placed above the culture such that the light intensity was between 80 and 110 μmol m^{-2} s^{-1} as measured using a Quantum meter (Apogee Instruments, Model MQ-510), which corresponds to placing the LED panels ~30 cm from the cultures. To control the light duty cycles, the LED panels were regulated with a Nearpow Multifunctional Infinite Loop Programmable Plug-in Digital Timer Switch.

To measure cell concentration, OD measurements were taken at 600 nm (OD_{600}), using medium (exposed to the same light and incubation conditions as the bacteria cultures) as the blank. Measurements were taken using a TECAN plate reader (infinite M200PRO, data stored in Microsoft Excel) or an Eppendorf spectrophotometer (BioSpectrometer basic) with a microvolume measuring cell (Eppendorf μCuvette G1.0), using samples diluted to a range of OD_{600} between 0.1 and 1.0.

Flow cytometry. Super-folder GFP (GFP) expression was quantified by flow cytometry using a BD LSR II flow cytometer (BD Biosciences) and BD FacsDiva 8.0.2 software, with an excitation wavelength of 488 nm and emission wavelength of 530 nm. The gating used in our analyses was defined to include positive (EMAL231) and negative (EMAL229) control cells based on GFP fluorescence, but exclude particles that were either too small or too large to be single living bacterial cells, based on side scatter (SSC-A) versus forward scatter (FSC-A) plots (Supplementary Fig. 4). Median fluorescence values were determined from 10,000 single-cell events. Single-cell events comprised at least 95% of total events for all samples.

The fluorescence data were normalized against the background fluorescence from cells lacking GFP (EMAL229) to account for potential light bleaching and cell autofluorescence. All fluorescence measurements were either taken at the end of the experiments or on aliquots taken from experimental cultures so that potential activation of YF1-FixJ by the light used to excite GFP did not affect the experiments or results. Because the superfolder GFP variant that we used folds in less than 5 min (ref. [53]), maturation time should not be a contributing factor in our fluorescence measurements.

Fermentation sample preparation and analytical methods. For mevalonate production, 560 μl of cell culture was mixed with 140 μl of 0.5 M HCl in a 1.5-ml microcentrifuge tube and vortexed at high speed for 1 min to convert mevalonate to (±)-mevalonolactone. The mixture was then centrifuged at 17,000 r.c.f. for 45 min at 4 °C in a benchtop centrifuge (Eppendorf Centrifuge 5424) to obtain cell-free supernatant. Then, 250 μl of this supernatant was transferred to an HPLC vial for analysis. For isobutanol production, 700 μl of cell culture was transferred to a 2-ml microcentrifuge tube and centrifuged as described above to obtain cell-free supernatant, then 250 μl of the supernatant was transferred to an HPLC vial for analysis.

Cell-free supernatant samples were analyzed via liquid chromatography (Agilent 1260 Infinity) using an Aminex HPX-87H ion-exchange column (Bio-Rad). The mobile phase was 5 mM sulfuric acid. Samples were run through the column at 55 °C and a flow rate of 0.6 ml min^{-1}. Mevalonate and isobutanol were monitored with a refractive index detector (RID, Agilent G1362A). To determine their concentration, the peak areas were measured using Agilent OpenLab CDS Chemstation software and compared to those of their own standard solutions for quantification, using (±)-mevalonolactone (Sigma-Aldrich) for mevalonate.

Sodium dodecyl sulfate polyacrylamide gel electrophoresis, western blotting and protein quantification. Samples were prepared by centrifuging 1-ml cell cultures at 17,000 r.c.f. for 5 min in a benchtop microcentrifuge (Thermo Scientific, Sorvall Legend Micro 17) at room temperature. The pellets were resuspended in 200 μl of resuspension buffer (Tris 50 mM, pH 8.0 and 300 mM NaCl), mixed with 50 μl of SDS sample buffer, and incubated at 100 °C in a heat block (Eppendorf ThermoMixer C) for 10 min at 700 r.p.m. Samples were loaded onto 12% SDS-PAGE gels and resolved. The volumes loaded on the gels (between 3 and 20 μl) were adjusted based on the OD_{600} measured just before the samples were harvested (between 0.5–3) to load the same amount of total cell mass, equivalent to 10 μl of sample from cells harvested at a final $OD_{600} = 1$.

Following electrophoresis, gels were either stained with Coomassie Brilliant Blue G-250 (Thermo Fisher), used as loading controls or analyzed by western blot following previously described methods[54]. Proteins were transferred onto PVDF membranes using a Trans-Blot Turbo Transfer System (Bio-Rad) using the standard protocol. LacI protein expression was assayed using a mouse anti-LacI antibody (Abcam, ab33832; 1/4,000) and goat anti-mouse secondary antibody (Abcam, ab205719; 1/10,000). YFP and FdeR expression were assayed using a mouse anti-His tag antibody (GenScript, A00612; 1/10,000). Blots were revealed using Clarity ECL substrate (Bio-Rad) according to the manufacturer's instructions. Images were taken using a Bio-Rad ChemiDoc MP Imaging System with Image Lab software, using the chemiluminescence protocol. Pixel intensity was quantified using ImageJ software (https://imagej.nih.gov/ij/). For all western blots, identically loaded gels were run and stained with Coomassie Brilliant Blue to confirm equal protein loading.

Construction of OptoLAC circuits. Deletion of *lacI* was performed using the Datsenko–Wanner method[55], using primers with 70 base pairs of homology to the promoter and terminator regions of the targeted gene. These primers were used to amplify the kanamycin resistance marker flanked by flippase recognition target (FRT) sites from pKD4, or the spectinomycin resistance marker from pYTK91[56]. Cells were made electrocompetent and electroporated as described previously[57]. FRT-flanked resistance markers were cured using flippase (FLP) recombinase from pCP20[58]. Gene deletions were genotyped by sequencing PCR products amplified from purified genomic DNA using primers flanking the region of deletion. A detailed description of all the strains used in this study is provided in Supplementary Table 2.

Strain MG1655 *ΔlacI::FRT-KanR-FRT* was obtained as a gift from M. Brynildsen[12]. From this strain, we removed the kanamycin resistance marker remaining from *lacI* deletion through FLP-FRT recombination. Hereafter, we call this strain OptoMG (EMAL52). Chemically competent OptoMG was transformed with pDawn controlling *lacI* (pMAL288) and a reporter plasmid containing $P_{T5\text{-}lacO}$-GFP (pMAL292) to make EMAL57. Three different SsrA tags with progressively weaker degradation strengths[14] (based on the last three residues) were added to the C terminus of LacI: LAA (pMAL294/OptoLAC1), AAV (pMAL296/OptoLAC2) and ASV (pMAL300). OptoMG was transformed with pMAL292 and each of these plasmids to make EMAL68, EMAL69 and EMAL71, respectively. To construct OptoLAC3, a *lacO* site was added between the P_{FixK2} promoter and its downstream ribosome-binding site in pMAL296 (see sequence in Supplementary Note 2), creating pMAL630. OptoMG was transformed with pMAL292 and pMAL630 to make EMAL230. Full sequences for OptoLAC1, 2 and 3 are available as Supplementary Notes 7, 8 and 9, respectively.

As controls for GFP measurement, we transformed OptoMG with pMAL630 (OptoLAC3) and pMAL207 (Empty vector), to produce EMAL229. This strain served as a negative control for subtraction of cell autofluorescence. In addition, we transformed OptoMG with pMAL630 (OptoLAC3) and pMAL301 (P_{BBA}-GFP), to produce EMAL231. This strain expresses GFP constitutively, serving as a positive control to check for photobleaching of GFP under blue light.

Characterization of OptoLAC circuits. To evaluate the response of our circuits to blue light, we inoculated 1-ml cultures of EMAL57, EMAL68, EMAL69, EMAL71, EMAL229, EMAL230 and EMAL231 and grew them overnight in M9 medium + 2% glucose + ampicillin + kanamycin at 37 °C and 200 r.p.m. under constant blue light to avoid premature transcription of GFP. The next day, we back-diluted the cultures into the same medium to $OD_{600} = 0.01$ in 150-μl triplicates into separate 96-well plates and grew the cultures for 8 h under blue light or in the dark (by wrapping the plate in aluminum foil). For light dose-response analysis, additional conditions of light were tested by applying light pulses of 10 s on/990 s off and 100 s on/900 s off. To evaluate the response to light intensity,

we used a rheostat (TerraBloom, VFSC) to adjust the panels to different light intensities, while keeping them at the same distance (~30 cm) from the cell cultures as in previous experiments. After growing for 8 h, 1 µl from each well was diluted into separate wells containing 199 µl of ice-cold phosphate buffered saline (PBS; Corning Life Sciences), kept on ice, and taken for flow cytometry analysis.

To characterize the induction of GFP expression from OptoLAC circuits in OptoMG strains with IPTG under blue light, we inoculated 1-ml overnight cultures (as above) of EMAL229, EMAL68, EMAL69 and EMAL230. The next day, we back-diluted the cultures to $OD_{600} = 0.01$ in 150-µl triplicates into separate 96-well plates, added IPTG to a final concentration of 0 µM, 1 µM, 5 µM, 10 µM, 100 µM or 1 mM, and grew the cultures for 8 h under blue light. Samples were then prepared as explained above and taken for flow cytometry analysis.

To analyze circuit performance at lower temperatures, we inoculated 1-ml overnight cultures of EMAL229, EMAL231, EMAL68, EMAL69 and EMAL230 (as above). The next day, we back-diluted the cultures to $OD_{600} = 0.01$ in 150 µl triplicates into separate 96-well plates and grew the cultures for 48 h under blue light or in the dark (by wrapping the plate in aluminum foil) at 18 °C. Samples were then taken for flow cytometry analysis (as above).

To test the performance of our circuits with different IPTG-inducible promoters, chemically competent OptoMG was transformed with pMAL294 (OptoLAC1) and one of the following two plasmids: a minimal-copy reporter plasmid containing P_{lacUV5}-GFP (pMAL302) or P_{trc}-GFP (pMAL303). We named these strains EMAL267 and EMAL268, respectively. We inoculated 1-ml overnight cultures of EMAL229, EMAL231, EMAL267 and EMAL268 (as above). The next day, we back-diluted the cultures to $OD_{600} = 0.01$ in 150-µl triplicates into separate 96-well plates and grew them for 8 h under blue light (pulses of 10 s on/990 s off and 100 s on/900 s off) or in the dark (by wrapping the plate in aluminum foil). Samples were then taken for flow cytometry analysis (as above).

To test different carbon sources, we inoculated 1-ml overnight cultures of EMAL229, EMAL231 and EMAL68 in M9 medium + 20 g l^{-1} glucose or xylose, LB medium (Miller) or SOB medium (at 37 °C and 200 r.p.m.). The next day, we back-diluted the cultures to $OD_{600} = 0.01$ in 150-µl triplicates into separate 96-well plates, and grew the cultures for 8 h under full blue light (light pulses of 10 s on/990 s off or 100 s on/900 s off) or in the dark (by wrapping the plate in aluminum foil). Samples were then taken for flow cytometry analysis (as above).

To quantify differences in LacI protein levels for OptoLAC1, OptoLAC2 and OptoLAC3, we inoculated 1-ml overnight cultures of EMAL68, EMAL69 and EMAL230 (as above). The next day, we back-diluted the cultures to $OD_{600} = 0.01$ in 1-ml triplicates into separate 24-well plates and grew the cultures for 8 h under blue light or in the dark (by wrapping the plate in aluminum foil). The OD_{600} of each sample was measured before harvesting the full 1-ml culture for western blot analysis.

To test spatial control of GFP expression, we inoculated a 1-ml overnight culture of EMAL68 (as above). The next day, 500 µl of culture was spread onto a 150 mm × 15 mm LB medium + kanamycin + ampicillin agar plate (Laboratory Disposable Products, catalog no. 229656-CT) using sterile glass beads. The plate was placed in ambient temperature on top of a black cloth and 35 cm underneath a projector (Epson H764A) displaying an image of a tiger (Drawing Work). The set-up was covered in black cloth to prevent ambient light contamination. After 16 h, the plate was imaged for GFP fluorescence using a Bio-Rad ChemiDoc MP Imaging System with Image Lab software, with Blue Epi illumination using a 530/28 filter (filter 4).

Kinetic analysis of OptoLAC circuits. We prepared an IPTG-inducible control strain that contained constitutively expressed *lacI* from a plasmid of the same copy number to our OptoLAC circuits by transforming OptoMG with pMAL292 and pET28a, creating strain EMAL77. We inoculated 1-ml overnight cultures of EMAL229, EMAL68, EMAL69, EMAL230 and EMAL77 (as above). The next day, we back-diluted the cultures to $OD_{600} = 0.01$ in 1-ml triplicates into eight separate 24-well plates and grew the cultures for ~4 h under blue light, at which point the cultures reached $OD_{600} = 0.9$. At this point, we collected samples from one plate (corresponding to $t = 0$ h). For strains EMAL229, EMAL68, EMAL69 and EMAL230, we induced six of the remaining seven plates by wrapping them in aluminum foil. For EMAL77, we instead induced by adding 1 mM IPTG to six of the remaining seven plates, to a final concentration of 1 mM. The final (eighth) plate was left in blue light (for EMAL77, without IPTG) for 12 h as a control. Every 2 h up to 12 h after induction, one plate was uncovered to measure the levels of GFP expression (and then discarded), by diluting 1 µl of culture into separate wells containing 199 µl of ice-cold PBS (Corning Life Sciences) and keeping on ice for flow cytometry analysis.

To explore the on-to-off kinetics, chemically competent OptoMG was transformed with either OptoLAC1, OptoLAC2 or OptoLAC3 and a minimal-copy reporter plasmid containing destabilized $P_{T5\text{-}lacO}$-GFP-SsrA-AAV (pMAL897). We named these strains EMAL343, EMAL344 and EMAL345, respectively. We inoculated 1-ml overnight cultures of EMAL229, EMAL343, EMAL344 and EMAL345 (as above). The next day, we back-diluted the cultures to $OD_{600} = 0.1$ in 1-ml triplicates into nine separate 24-well plates and grew the cultures for ~3 h in darkness (by wrapping them in aluminum foil), at which point the cultures reached $OD_{600} = 0.9$. At this point, we collected samples from one plate (corresponding to $t = 0$ h). We then repressed (uninduced) four of the remaining eight plates by removing them from foil and culturing them under constant blue light. The remaining four plates were left in darkness as controls. Every 1.5 h up to 6 h after induction, one plate from each condition was uncovered to measure the levels of GFP expression (and then discarded), by diluting 1 µl of culture into separate wells of a 96-well plate containing 199 µl of ice-cold PBS (Corning Life Sciences), and kept on ice for flow cytometry analysis.

Growth effects of OptoLAC circuits. To determine if our OptoLAC circuits impact cell growth in *E. coli* K strains, we inoculated 1-ml overnight cultures of EMAL68, EMAL69, EMAL230 and EMAL77 (as above). The next day, we back-diluted the cultures to $OD_{600} = 0.01$ in 1-ml triplicates into three separate 24-well plates. At this point, one plate was grown under continuous blue light (for EMAL77, without IPTG) for 12 h, one plate was grown in darkness (for EMAL77, with 1 mM IPTG) for 12 h, and one plate was grown under blue light for 4 h, then switched to darkness for 8 h (for EMAL77, without IPTG for 4 h, then with 1 mM IPTG for 8 h). OD_{600} measurements were taken every 2 h from the time of inoculation.

Construction of isobutanol-producing strains. We transformed chemically competent OptoMG cells with either OptoLAC1, OptoLAC2 or OptoLAC3 and a plasmid that combines all the genes from pSA65 and pSA69 in a single vector with a p15A origin of replication and β-lactamase resistance marker (pMAL534), generating strains EMAL199, EMAL200 and EMAL239, respectively. A light-insensitive IPTG-inducible control strain was made by co-transforming chemically competent OptoMG with pMAL534 and pET28a, generating EMAL201 (Supplementary Table 1). These strains (EMAL199, EMAL200, EMAL239 and EMAL201) express (from the P_{L_lacO1} promoter) three enzymes that convert pyruvate to 2-ketoisovalerate: acetolactate synthase from *Bacillus subtilis* (*BsalsS*), acetohydroxyacid reductoisomerase (*ilvC*) and dihydroxyacid dehydratase (*ilvD*). They also express, from another P_{L_lacO1} promoter, two enzymes that convert 2-ketoisovalerate into isobutanol: 2-ketoacid decarboxylase from *Lactococcus lactis* (*Llkivd*) and alcohol dehydrogenase from *Lactococcus lactis* (*LladhA*). The transformants were plated on LB medium + kanamycin + ampicillin agar and colonies were grown under blue light to avoid negative selection due to the potential pathway expression. Four colonies from each strain were screened for isobutanol production. Each colony was used to inoculate 1 ml of M9 + 2% glucose + kanamycin + carbenicillin medium, grown overnight at 37 °C and 200 r.p.m. under blue light. The next day, each culture was back-diluted into the same medium to an OD_{600} of 0.01 and grown for 4 h at 37 °C at 200 r.p.m. under blue light. The plates were then sealed with Nunc Sealing Tape (Thermo Scientific) and wrapped in aluminum foil; for the control strain EMAL201, IPTG was added to 1 mM before sealing and wrapping. No holes were poked in the sealing tape to prevent evaporation of isobutanol. The strains were fermented in the dark at 30 °C at 200 r.p.m. for 72 h, after which samples were prepared for HPLC analysis as described above. The highest-producing colonies were selected for subsequent optimization.

To find the optimal value of ρ_s for isobutanol production, we back-diluted 1-ml overnight cultures of each strain to different OD_{600} values (ranging from 0.001 to 0.1) in 1-ml cultures of the same media described above (in quadruplicates). The different dilutions were grown for 4 h, reaching different OD_{600} values, at which time cultures were switched from light to dark conditions (values in Fig. 3b,c), or induced with IPTG (Extended Data Fig. 8a). As controls, we grew each strain under continuous blue light (EMAL199, EMAL200, EMAL239) or with no IPTG added (EMAL201). The same fermentation procedure described above was then followed.

Construction of mevalonate-producing strains. We transformed chemically competent OptoMG cells with either OptoLAC1, OptoLAC2 or OptoLAC3 and a modified version of pMevT[18] in which P_{lac} was replaced with P_{lacUV5} (pMAL487), generating strains EMAL208, EMAL209 and EMAL235, respectively. A light-insensitive IPTG-inducible control strain was made by transforming chemically competent OptoMG cells with pMAL487 and pET28a, generating EMAL135 (Supplementary Table 1). These strains (EMAL208, EMAL209, EMAL235 and EMAL135) express, from a single operon, the first three enzymes of the mevalonate pathway, which convert acetyl-CoA into mevalonate: acetoacetyl-CoA thiolase (*atoB*) from *E. coli*, 3-hydroxy-3-methylglutaryl-CoA synthase (HMGS or *ERG13*) from *S. cerevisiae*, and a truncated version of 3-hydroxy-3-methylglutaryl-CoA reductase (tHMGR) from *S. cerevisiae*. The transformants were plated on LB + kanamycin + chloramphenicol agar and colonies were grown under blue light to avoid potential negative selection due to pathway expression. Four colonies from each strain were screened for mevalonate production. Each colony was used to inoculate 1 ml of M9 + 2% glucose + chloramphenicol + kanamycin medium, grown in a 24-well plate overnight at 37 °C and 200 r.p.m. under blue light. The next day, each culture was back-diluted into the same medium to an OD_{600} of 0.01 and grown for 4 h at 37 °C at 200 r.p.m. under blue light. The plates were then sealed with Nunc Sealing Tape (Thermo Scientific) and wrapped in aluminum foil; for the control strain EMAL135, IPTG was added to 1 mM before sealing and wrapping. A single

hole (using a sterile syringe needle) was poked in the center of the sealing tape covering each sample well to allow limited aeration. The strains were fermented in the dark at 37 °C at 200 r.p.m. for 72 h, after which samples were prepared for HPLC analysis as described above. The highest-producing colonies were selected for subsequent optimization.

To find the optimal value of ρ_s for mevalonate production, we back-diluted 1-ml overnight cultures of each strain to different OD_{600} values (ranging from 0.001 to 0.1) in 1-ml cultures of the same media as described above (in quadruplicates). The different dilutions were grown for 4 h, reaching different OD_{600} values, at which time cultures were switched from light to dark conditions (values in Fig. 4b,c) or induced with IPTG (Extended Data Fig. 8b). As controls, we grew each strain under continuous blue light (EMAL208, EMAL209, EMAL235) or with no IPTG added (EMAL135). The same fermentation procedure described above was then followed.

Scale-up of chemical production in a 2-l bioreactor. To validate our circuits for chemical production in higher cell density conditions and larger culture volumes, we grew a 5-ml overnight culture of EMAL208 (OptoLAC1 driving mevalonate production) in M9 + 5% glucose + kanamycin + chloramphenicol under blue light at 37 °C. We then set up a BioFlo120 system with a 2-l bioreactor (Eppendorf, B120110001) and added 1 l of sterile M9 + 5% glucose + kanamycin + chloramphenicol. The reactor was set to 37 °C, pH 7.0 (which was maintained using a base feed of ammonium hydroxide (Thomas Scientific), and a minimum dissolved oxygen percentage of 20 (maintained by adjusting the agitation rate between 200 and 800 r.p.m. and by injecting air at a flow rate of 0.1–3.0 SLPM (standard litres per minute)). Three blue LED panels were placed in a triangular formation ~20 cm from the reactor such that the light illuminated ~76% of the bulk surface area at an intensity of 80–110 μmol m^{-2} s^{-1} (Supplementary Fig. 2). The reactor was then inoculated to an OD_{600} of 0.004, and the cells were grown for ~4 h under blue light until reaching an OD_{600} of 0.17. The lights were then turned off and the reactor was wrapped in aluminum foil and covered with black cloth. At 8 h, 50 μl of Antifoam 204 (Sigma-Aldrich) was added to prevent foaming. Culture samples of 1 ml were taken while minimizing potential exposure of the culture to ambient light and prepared for HPLC analysis as described above.

Protein production. To develop strains for protein production, we knocked out the endogenous copy of *lacI* from BL21 DE3 and removed the remaining kanamycin resistance marker left by the knockout (as described above), resulting in EMAL224. We then deleted the copy of *lacI* introduced by the DE3 prophage, resulting in EMAL255. We call this strain OptoBL in this study. For YFP production, we transformed electrocompetent OptoBL cells with pMAL658 (OptoLAC1B) and pC85 (P_{T7}-YFP), resulting in EMAL284. As an IPTG-inducible control containing constitutive *lacI*, we transformed BL21 DE3 with pCri-8b[21] (P_{T7}-YFP, P_{lacIQ}_*lacI*), resulting in EMAL283. For FdeR production, we transformed electrocompetent OptoBL cells with one of pMAL658 (OptoLAC1B) or pMAL659 (OptoLAC2B), as well as pMAL887 (P_{T7}-FdeR), resulting in EMAL335 and EMAL336, respectively. As an IPTG-inducible control, we transformed BL21 DE3 with pC9 (P_{T7}-FdeR, P_{lacIQ}_*lacI*), which contains constitutive *lacI*, resulting in EMAL329. Transformation agar plates for light-sensitive strains were grown under constant blue light to avoid negative selection due to protein expression.

To determine if our OptoLAC circuits impact cell growth in *E. coli* B strains (OptoBL), we inoculated 1-ml overnight cultures of EMAL276, EMAL283, and EMAL284 in LB medium and their appropriate selection antibiotics (EMAL284 also in blue light). The next day, we back-diluted the cultures to OD_{600} = 0.01 in 1-ml triplicates into two separate 24-well plates. One plate was grown under continuous blue light (for EMAL276 and EMAL283, without IPTG) for 15 h; the other plate was grown under blue light for 4 h, then switched to darkness for 11 h (for EMAL283, without IPTG for 4 h, then with 1 mM IPTG for 11 h). In both plates, we grew additional triplicates of EMAL284 that were induced with 1 mM IPTG after 4 h of growth. OD_{600} measurements were taken every 2 h from the time of inoculation.

For kinetic analysis of protein production, we inoculated 1-ml overnight cultures of EMAL283, EMAL329, EMAL284 and EMAL336 in LB medium and their appropriate selection antibiotics (EMAL284 and EMAL336 also in blue light). The next day, we back-diluted the cultures to OD_{600} = 0.03 in 1-ml cultures into eight separate 24-well plates and grew the cultures to OD_{600} = 0.5 (which took ~3 h) under blue light. We then switched seven of the plates to the dark by wrapping them in aluminum foil, adding IPTG to a final concentration of 1 mM for EMAL283 and EMAL329. One plate was left in blue light and without IPTG for 12 h as a control. The OD_{600} of each sample was measured before harvesting the full 1-ml culture at 0 h, 1 h, 2 h, 3 h, 6 h, 9 h and 12 h for analysis.

To find the optimal ρ_s value for protein production, we inoculated 1-ml overnight cultures of EMAL283, EMAL329, EMAL284 and EMAL336 (as above). The next day, we back-diluted the cultures to OD_{600} values between 0.01 and 0.1 in 1-ml cultures into a 24-well plate and grew the cultures to OD_{600} values between 0.1 and 1.8 (which took ~3 h) under blue light. We then induced protein expression by switching the plate to the dark (wrapping it in aluminum foil) or by adding IPTG to a final concentration of 1 mM for EMAL283 and EMAL329. As controls, we grew cultures that were kept under blue light/without IPTG for the duration of the experiment (non-induced), as well as cultures of EMAL284 and EMAL336 that were induced with 1 mM IPTG after 3 h of growth but kept under blue light. The OD_{600} of each sample was measured before harvesting the full 1-ml culture at 9 h for analysis.

To test tunability of protein production using different exposures to light or IPTG concentrations, we inoculated 1-ml overnight cultures of EMAL283, EMAL329, EMAL284 and EMAL336 (as above). The next day, we back-diluted the cultures to OD_{600} = 0.01 for YFP or OD_{600} = 0.03 for FdeR in 1-ml cultures into six separate 24-well plates and grew the cultures to OD_{600} = 0.1 for YFP or OD_{600} = 0.5 for FdeR (which took ~3 h) under blue light. We then moved the plates to six separate light conditions: full blue light; pulses of 1 s on/999 s off, 5 s on/995 s off, 10 s on/990 s off, 100 s on/900 s off; or in the dark (by wrapping the plate in aluminum foil). For EMAL283 and EMAL329, we back-diluted the cultures to OD_{600} = 0.01 for YFP or OD_{600} = 0.03 for FdeR in 1-ml cultures into a 24-well plate and grew the cultures to OD_{600} = 0.1 for YFP or OD_{600} = 0.5 for FdeR (which took ~3 h). We then added IPTG to final concentrations of 0 μM, 1 μM, 10 μM, 100 μM, 500 μM and 1 mM. The OD_{600} of each sample was measured before harvesting the full 1-ml culture at 9 h for analysis.

Statistics. Statistical significance was determined using a standard *t*-test for *P* values. The *t* scores were calculated by the formula $\frac{(\mu_{condition1}-\mu_{condition2})\sqrt{N}}{\sigma_{condition2}}$. *P* values were calculated using a degree of freedom of $N-1$ and a two-sided *t*-test calculator.

Reporting Summary. Further information on research design is available in the Nature Research Reporting Summary linked to this Article.

Data availability

All data supporting the findings of this study are available within the paper and Supplementary Information. Source data are provided with this paper.

References

49. Inoue, H., Nojima, H. & Okayma, H. High efficiency transformation of *Escherichia coli* with plasmids. *Gene* **96**, 23–28 (1990).
50. Gibson, D. G. et al. Enzymatic assembly of DNA molecules up to several hundred kilobases. *Nat. Methods* **6**, 343–345 (2009).
51. Atsumi, S. et al. Engineering the isobutanol biosynthetic pathway in *Escherichia coli* by comparison of three aldehyde reductase/alcohol dehydrogenase genes. *Appl. Microbiol. Biotechnol.* **85**, 651–657 (2010).
52. Zhou, K., Qiao, K., Edgar, S. & Stephanopoulos, G. Distributing a metabolic pathway among a microbial consortium enhances production of natural products. *Nat. Biotechnol.* **33**, 377–383 (2015).
53. Pédelacq, J. D., Cabantous, S., Tran, T., Terwilliger, T. C. & Waldo, G. S. Engineering and characterization of a superfolder green fluorescent protein. *Nat. Biotechnol.* **24**, 79–88 (2006).
54. Towbin, H., Staehellin, T. & Gordon, J. Electrophoretic transfer of proteins from polyacrylamide gels to nitrocellulose sheets: procedure and some applications. *Proc. Natl Acad. Sci. USA* **76**, 4350–4354 (1979).
55. Datsenko, K. A. & Wanner, B. L. One-step inactivation of chromosomal genes in *Escherichia coli* K-12 using PCR products. *Proc. Natl Acad. Sci. USA* **97**, 6640–6645 (2000).
56. Lee, M. E., DeLoache, W. C., Cervantes, B. & Dueber, J. E. A highly characterized yeast toolkit for modular, multipart assembly. *ACS Synth. Biol.* **4**, 975–986 (2015).
57. Dower, W. J., Miller, J. F. & Ragsdale, C. W. High efficiency transformation of *E. coli* by high voltage electroporation. *Nucleic Acids Res.* **16**, 6127–6145 (1988).
58. Cherepanov, P. P. & Wackernagel, W. Gene disruption in *Escherichia coli*: TcR and KmR cassettes with the option of Flp-catalyzed excision of the antibiotic-resistance determinant. *Gene* **158**, 9–14 (1995).

Acknowledgements

We thank M. Brynildsen for strain MG1655 *ΔlacI::FRT-KanR-FRT*, A. Möglich for plasmids pDusk and pDawn, J. Keasling for plasmid pMevT and J. Liao for plasmids pSA65 and pSA69. We are very grateful to W. Mok and M. Brynildsen for advice and troubleshooting regarding *E. coli* protocols. We thank C. DeCoste, K. Rittenbach and the Princeton Molecular Biology Flow Cytometry Resource Center for assistance with flow cytometry experiments. J.L.A. is supported by the US Department of Energy, Office of Science, Office of Biological and Environmental Research award no. DE-SC0019363, the NSF CAREER Award CBET-1751840, The Pew Charitable Trusts, The Eric and Wendy Schmidt Transformative Technology Fund Award and the Camille Dreyfus Teacher-Scholar Award.

Author contributions

M.A.L. and J.L.A. conceived this project and designed the experiments. M.A.L., S.S.I. and C.C.-L. constructed the strains and plasmids. M.A.L. and S.S.I. performed the experiments shown in Figs. 1 and 2. M.A.L., E.M.Z. and H.K. performed the experiments shown in Figs. 3 and 4. M.A.L., C.C.-L. and C.D. performed the experiments shown in Fig. 5. M.A.L. performed experiments shown in Extended Data Figs. 1–10. C.C.-L. and C.D. performed experiments shown in Extended Data Figs. 2

and 9. M.A.L., C.C.-L. and J.L.A. analyzed the data and wrote the manuscript. J.L.A. supervised and funded the project.

Competing interests

J.L.A., M.A.L. and C.C.-L. have filed a patent application ('Optogenetic circuits for controlling chemical and protein production in *Escherichia coli*', US patent application 62,935,267) describing the OptoLAC circuit design and application for chemical and recombinant protein production.

Additional information

Extended data is available for this paper at https://doi.org/10.1038/s41589-020-0639-1.

Supplementary information is available for this paper at https://doi.org/10.1038/s41589-020-0639-1.

Correspondence and requests for materials should be addressed to J.L.A.

Reprints and permissions information is available at www.nature.com/reprints.

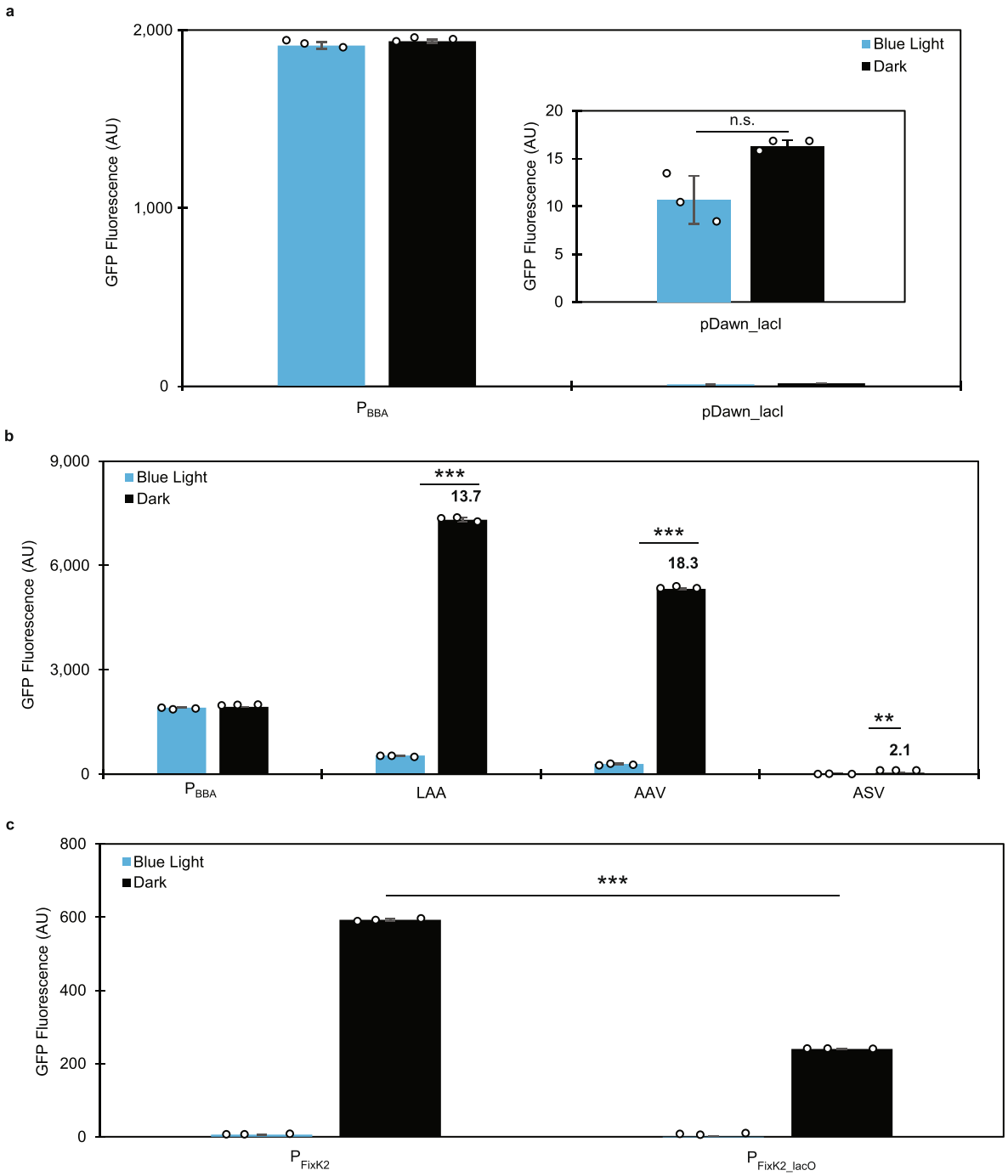

Extended Data Fig. 1 | Development of OptoLAC circuits. a, GFP expression in blue light or darkness from the constitutive P_{BBA} promoter (EMAL231) or from $P_{T5\text{-}lacO}$ in a strain in which *lacI* expression is controlled by pDawn (EMAL57). P = 0.07118. **b**, GFP expression in blue light or darkness from P_{BBA} (EMAL231) or from $P_{T5\text{-}lacO}$ in strains containing the pDawn system controlling LacI fused to SsrA tags terminating in LAA (EMAL68, which gave rise to OptoLAC1), AAV (EMAL69, which gave rise to OptoLAC2), or ASV (EMAL71). From left to right: P < 0.00001, P < 0.00001, P = 0.00536. **c**, GFP expression in blue light or darkness driven by the P_{FixK2} (pMAL441) or $P_{FixK2\text{-}lacO}$ (pMAL442) promoter using pDusk (EMAL152 and EMAL153, respectively). P = 0.000037. $^{**}P < 0.01$, $^{***}P < 0.001$. Statistics are derived using a two-sided *t*-test. All data shown as median values of 10,000 single-cell flow cytometry events; error bars represent one standard deviation of n = 3 biologically independent samples; open circles represent individual data points. Data are representative of n = 3 independent experiments.

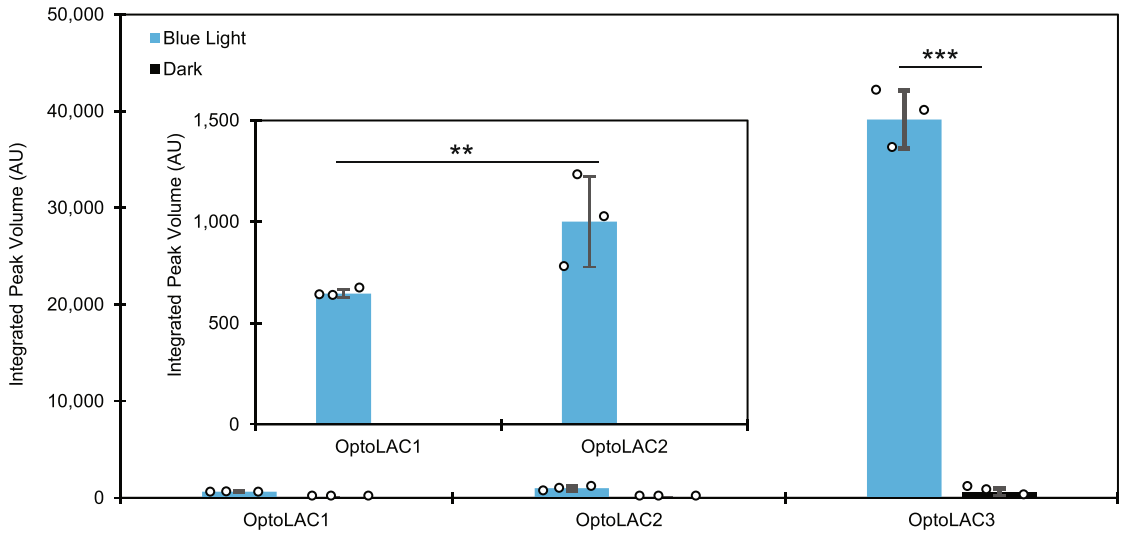

Extended Data Fig. 2 | Quantification of LacI protein levels for OptoLAC circuits. Integrated peak volumes of LacI protein levels quantified via Western blot. From left to right: P = 0.00102, P = 0.000041. Loading controls and uncropped blots used for quantification (samples derived from the same experiment and processed in parallel) are provided as source data. ** P < 0.01, ***P < 0.001. Statistics are derived using a two-sided *t*-test. All data shown as mean values; error bars represent the standard deviation of n = 3 biologically independent samples; open circles represent individual data points. Data are representative of n = 2 independent experiments.

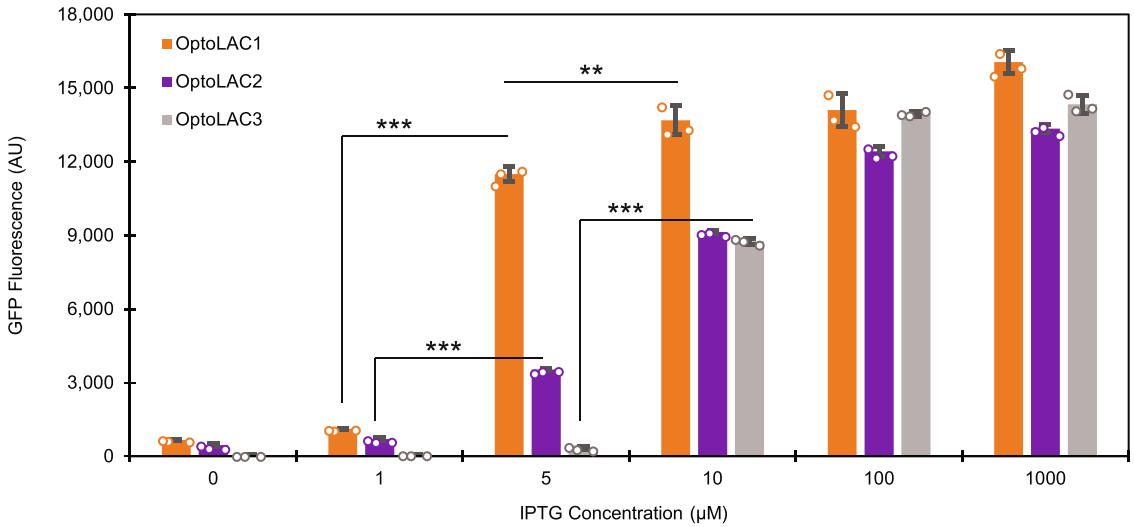

Extended Data Fig. 3 | Response of OptoLAC circuits to IPTG. GFP expression from $P_{T5\text{-}lacO}$ controlled by OptoLAC1 (orange, EMAL68), OptoLAC2 (purple, EMAL69), or OptoLAC3 (gray, EMAL230) under blue light with different concentrations of IPTG added at the time of inoculation. From left to right: P < 0.00001, P = 0.000076, P = 0.00692, P = 0.000025. $^{**}P < 0.01$, $^{***}P < 0.001$. Statistics are derived using a two-sided *t*-test. All data shown as median values of 10,000 single-cell flow cytometry events; error bars represent one standard deviation of n = 3 biologically independent samples; open circles represent individual data points. Data are representative of n = 3 independent experiments.

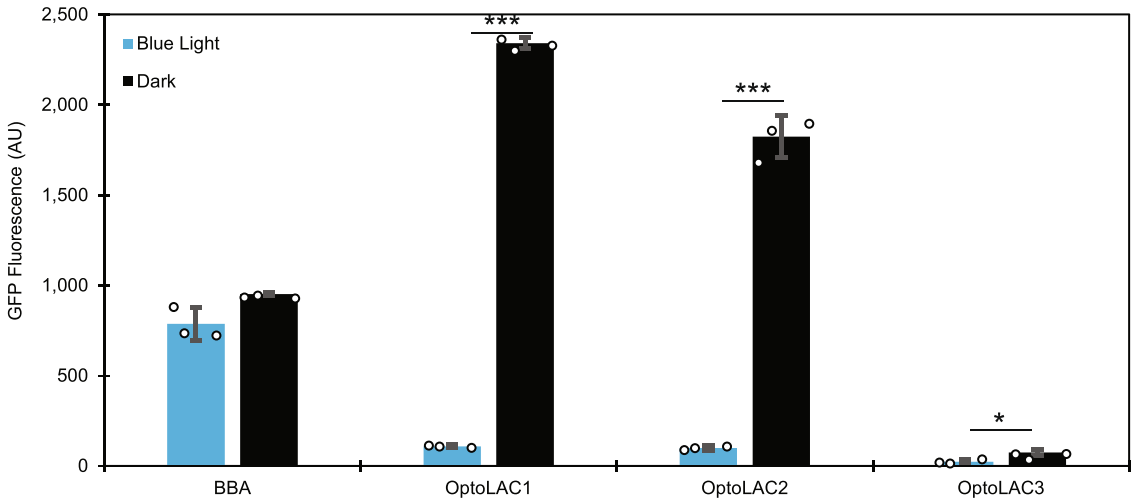

Extended Data Fig. 4 | Response of OptoLAC circuits to low temperatures. GFP expression at 18 °C from P_{BBA} (EMAL231) or $P_{T5\text{-}lacO}$ controlled by OptoLAC1 (EMAL68), OptoLAC2 (EMAL69), or OptoLAC3 (EMAL230) under blue light or darkness. From left to right: $P < 0.00001$, $P = 0.000014$, $P = 0.0222$. $^{*}P < 0.05$, $^{***}P < 0.001$. Statistics are derived using a two-sided *t*-test. All data shown as median values of 10,000 single-cell flow cytometry events; error bars represent one standard deviation of n = 3 biologically independent samples; open circles represent individual data points. Data are representative of n = 3 independent experiments.

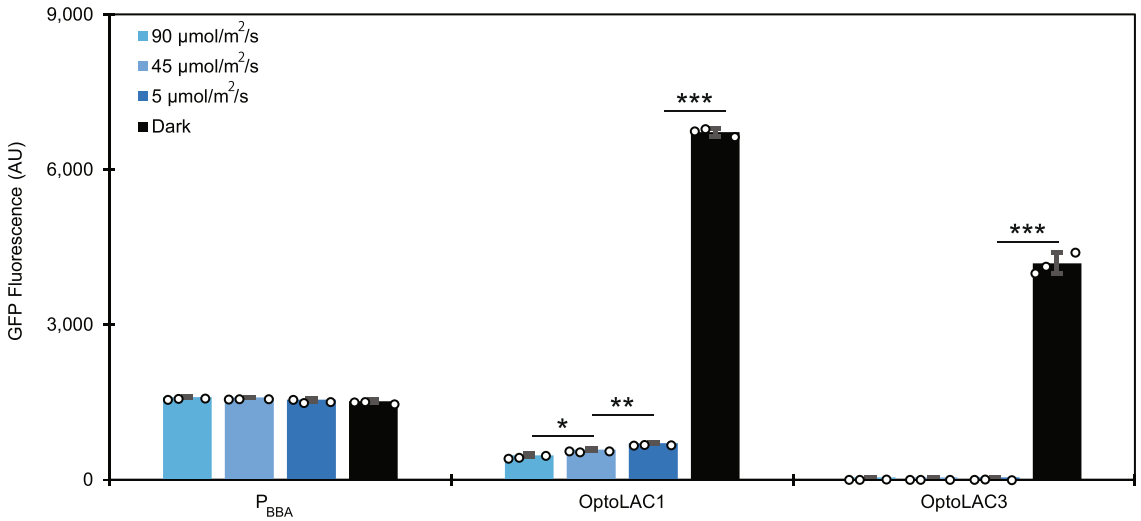

Extended Data Fig. 5 | Tunability of OptoLAC circuits with light intensity. GFP expression from the constitutive P_{BBA} promoter (EMAL231) or from $P_{T5\text{-}lacO}$ controlled by OptoLAC1 (EMAL68) or OptoLAC3 (EMAL230) under continuous blue light of differing intensities or darkness. From left to right: P = 0.0189, P = 0.00314, P < 0.00001, P < 0.00001. *$P < 0.05$, **$P < 0.01$, ***$P < 0.001$. Statistics are derived using a two-sided *t*-test. All data shown as median values of 10,000 single-cell flow cytometry events; error bars represent one standard deviation of n = 3 biologically independent samples; open circles represent individual data points. Data are representative of n = 3 independent experiments.

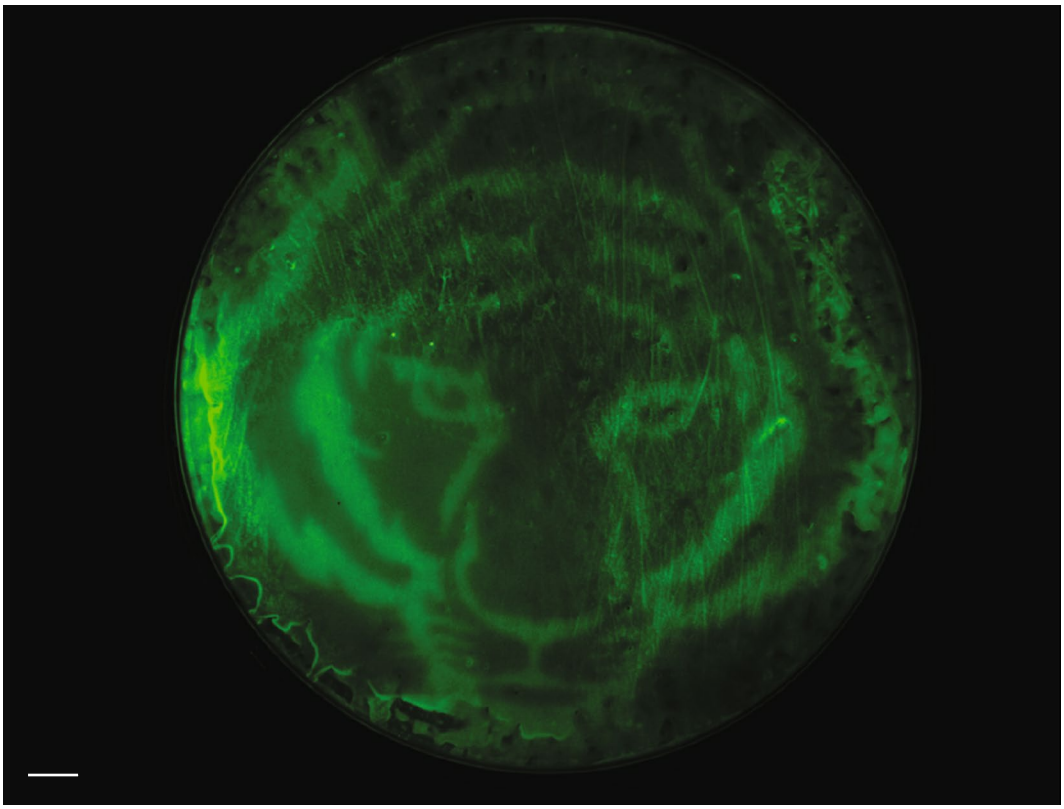

Extended Data Fig. 6 | Spatial control of GFP expression on an LB agar plate. LB agar plate containing a lawn of EMAL68 (OptoLAC1 driving GFP) illuminated with a projection of a tiger image. Scale bar: 1 cm. Data are representative of n = 2 independent experiments.

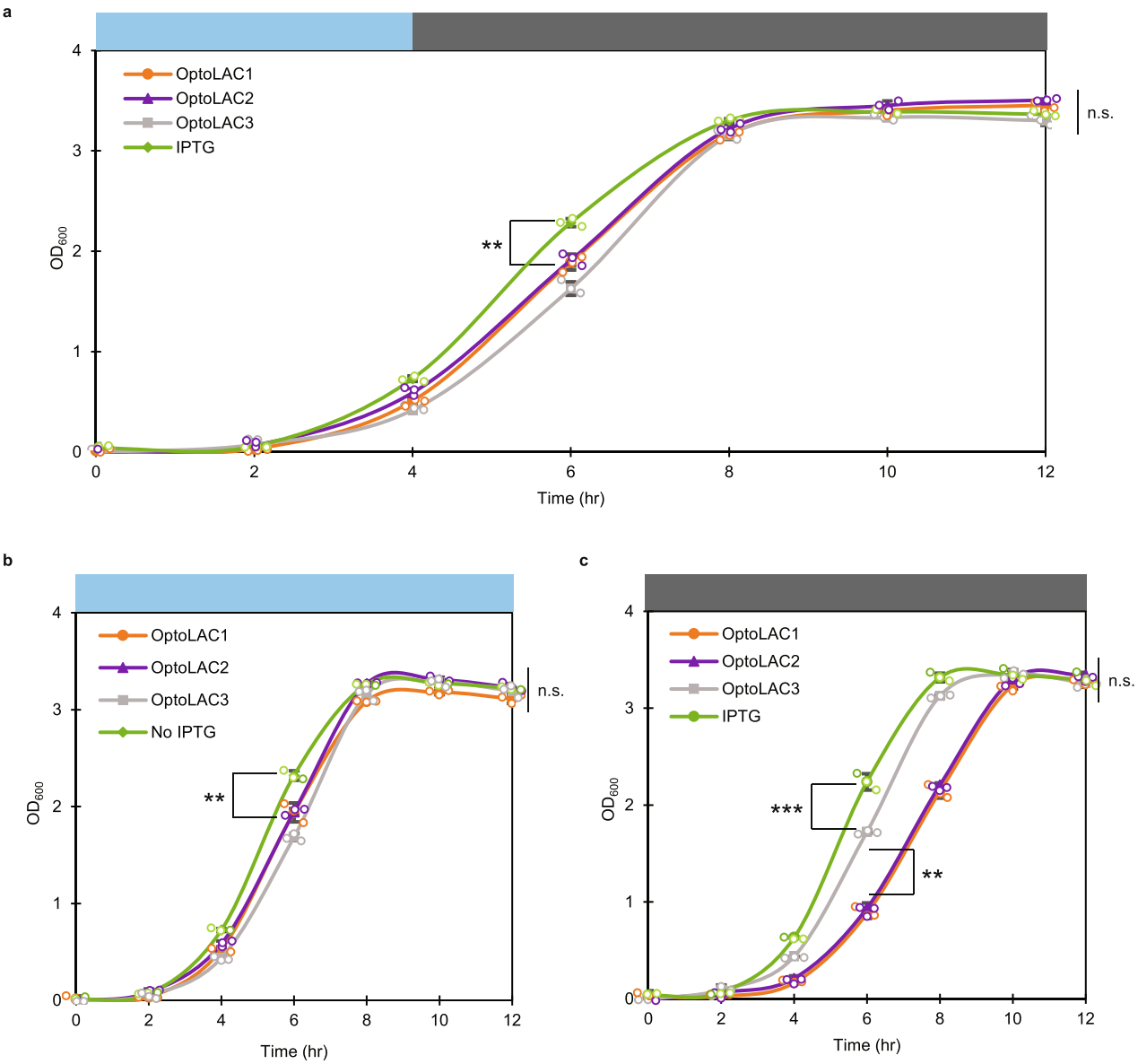

Extended Data Fig. 7 | Growth curves of K strains containing OptoLAC circuits under different induction conditions. a–c, OD_{600} measurements for strains containing OptoLAC1 (EMAL68; orange circle), OptoLAC2 (EMAL69; purple triangle), OptoLAC3 (EMAL230; gray square), or an IPTG-induced control (EMAL77; green diamond) using different induction conditions, shown on top of each graph as uninduced (blue) or induced (gray). **a**, Cultures of each strain grown under continuous blue light for 4 hours before switching them to darkness (OptoLAC circuits) or adding 1 mM IPTG (IPTG control). From left to right: P = 0.00827, P = 0.1472. **b**, Cultures grown entirely uninduced under continuous blue light (OptoLAC circuits) or without IPTG (IPTG control). From left to right: P = 0.00275, P = 0.0508. **c**, Cultures grown constitutively induced in darkness (OptoLAC circuits) or with 1 mM IPTG (IPTG control). From left to right: P = 0.000393, P = 0.00145, P = 0.33. $^{**}P < 0.01$, $^{***}P < 0.001$. Statistics are derived using a two-sided *t*-test. All data shown as mean values; error bars represent the standard deviation of n = 3 biologically independent samples; open circles represent individual data points. Data are representative of n = 2 independent experiments.

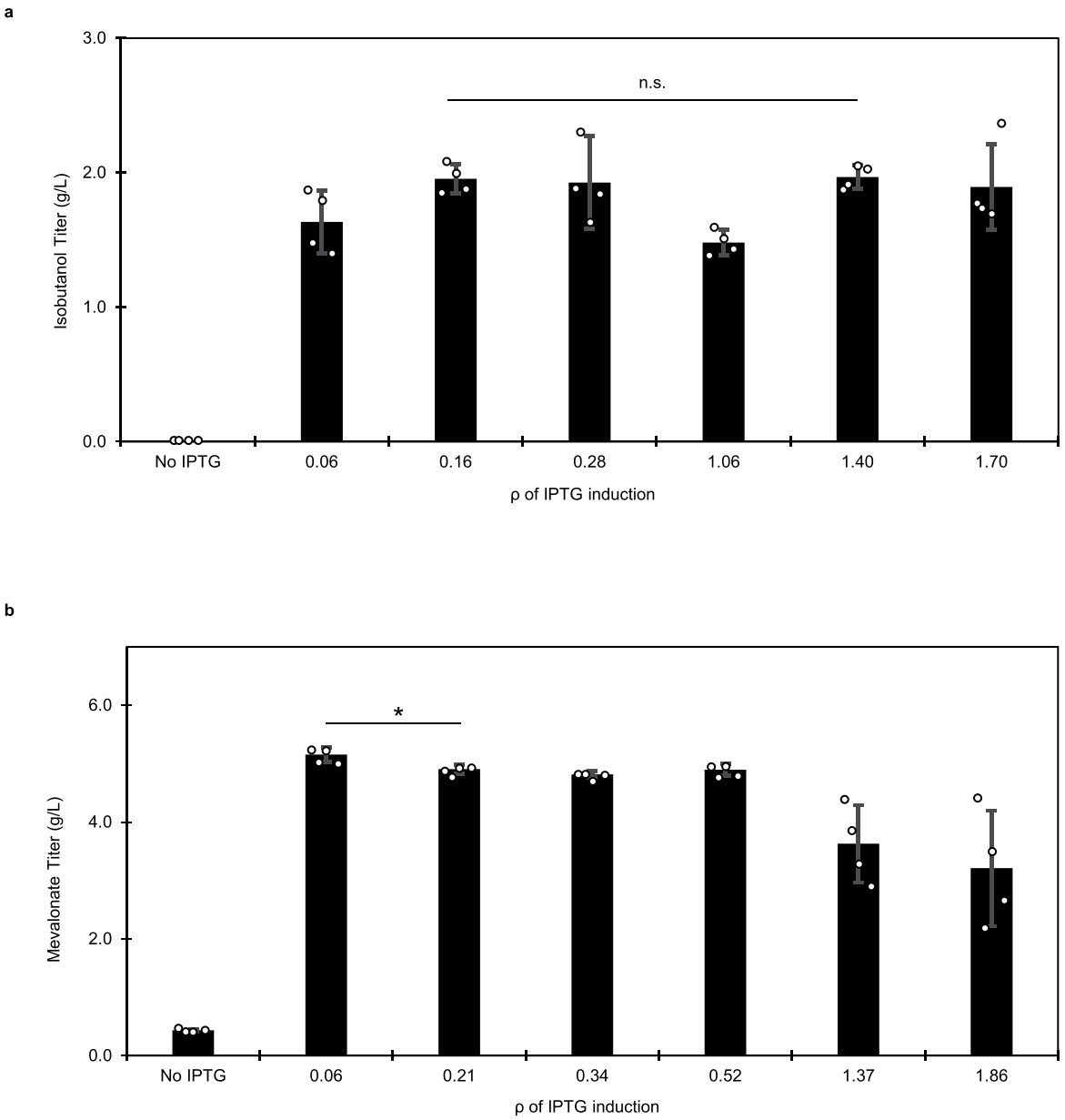

Extended Data Fig. 8 | Optimization of the cell density of induction with IPTG for chemical production. a, Isobutanol production from pMAL534 by EMAL201 when induced with 1 mM IPTG at different cell densities. P = 0.819. **b**, Mevalonate production from pMAL487 by EMAL135 when induced with 1 mM IPTG at different cell densities. P = 0.02185. *$P < 0.01$. Statistics are derived using a two-sided *t*-test. All data shown as mean values; error bars represent the standard deviation of n = 4 biologically independent samples; open circles represent individual data points. Data are representative of n = 2 independent experiments.

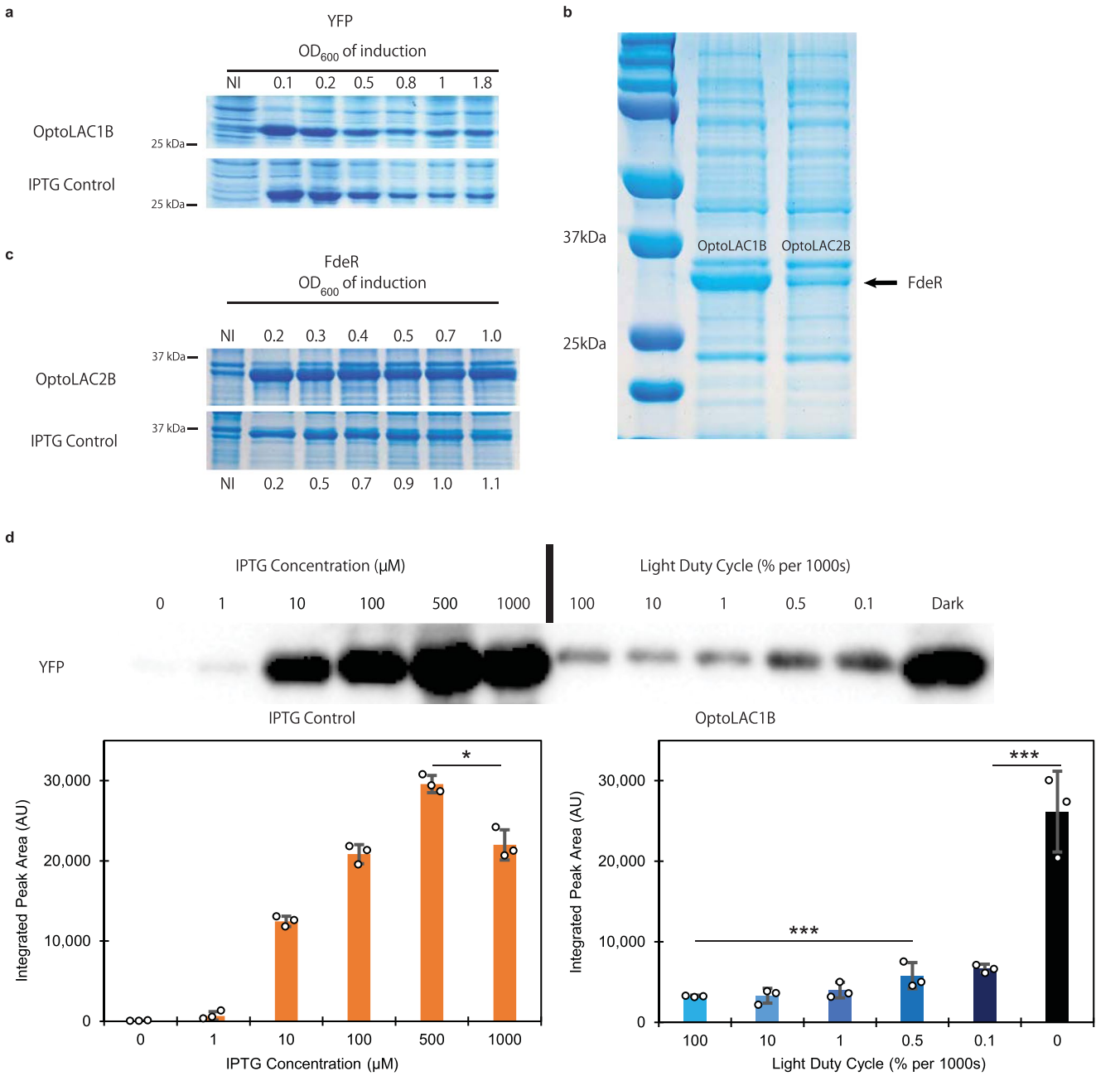

Extended Data Fig. 9 | Optimization of YFP and FdeR production using OptoLAC circuits. a, YFP production when inducing at different cell densities (ρ_s) by switching cultures from blue light to darkness using OptoLAC1B (EMAL284, top panel) or adding IPTG (EMAL283, bottom panel). NI = Not induced: kept under blue light or no IPTG added. **b**, Comparison of FdeR production between OptoLAC1B (EMAL335) and OptoLAC2B (EMAL336) cultured under continuous blue light for 12 hours. **c**, FdeR production when inducing at different cell densities (ρ_s) by adding IPTG (EMAL329, top panel) or switching cultures from blue light to darkness using OptoLAC2B (EMAL336, bottom panel). NI = Not induced: kept under blue light or no IPTG added. All samples were resolved via SDS-PAGE (12% polyacrylamide). **d**, Tunability of YFP production using different doses of light or concentrations of IPTG, resolved and quantified via Western blot. From left to right: P = 0.0201, P = 0.000383, P = 0.000206. Loading controls and uncropped gels and blots, including those used for quantification in **d** (samples derived from the same experiment and processed in parallel) are provided as source data. $^*P < 0.05$, $^{***}P < 0.001$. Statistics are derived using a two-sided *t*-test. All data shown as mean values; error bars represent the standard deviation of three biologically independent samples; open circles represent individual data points. Data are representative of n = 2 independent experiments.

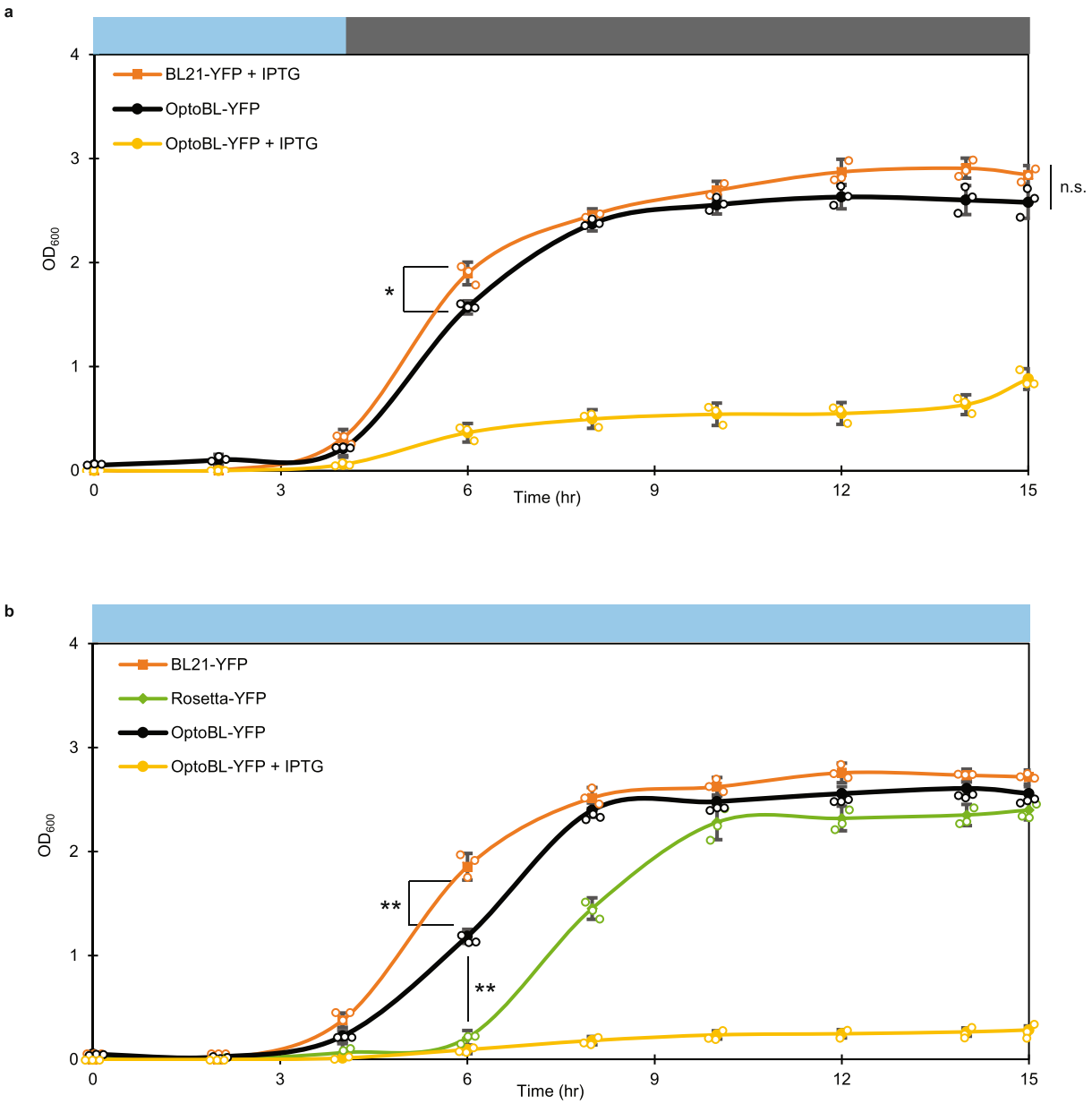

Extended Data Fig. 10 | Growth curves of B strains containing OptoLAC circuits under different induction conditions. a, **b**, Time course of OD_{600} readings for BL21 DE3 (EMAL283; orange square), Rosetta 2 (EMAL276; green diamond), and OptoBL containing OptoLAC1B (EMAL284; black circle without IPTG, yellow circle with IPTG), containing plasmids for YFP production, grown under different induction conditions, which are shown on top of each graph as uninduced (blue) or induced (gray). **a**, Cultures from each strain grown under blue light before switching to the dark (OptoLAC1B) or adding IPTG. From left to right: $P < 0.0122$, $P = 0.0946$. **b**, Cultures grown entirely uninduced under blue light (OptoLAC1B), without IPTG, or OptoLAC1B with blue light and IPTG. From left to right: $P = 0.00342$, $P = 0.0017$. $^{*}P < 0.05$, $^{**}P < 0.01$. Statistics are derived using a two-sided *t*-test. All data shown as mean values; error bars represent the standard deviation of n = 3 biologically independent samples; open circles represent individual data points. Data are representative of n = 2 independent experiments.

nature research

Corresponding author(s): Jose L. Avalos

Last updated by author(s): 7/3/2020

Reporting Summary

Nature Research wishes to improve the reproducibility of the work that we publish. This form provides structure for consistency and transparency in reporting. For further information on Nature Research policies, see Authors & Referees and the Editorial Policy Checklist.

Statistics

For all statistical analyses, confirm that the following items are present in the figure legend, table legend, main text, or Methods section.

n/a	Confirmed	
☐	☒	The exact sample size (*n*) for each experimental group/condition, given as a discrete number and unit of measurement
☐	☒	A statement on whether measurements were taken from distinct samples or whether the same sample was measured repeatedly
☐	☒	The statistical test(s) used AND whether they are one- or two-sided *Only common tests should be described solely by name; describe more complex techniques in the Methods section.*
☒	☐	A description of all covariates tested
☒	☐	A description of any assumptions or corrections, such as tests of normality and adjustment for multiple comparisons
☐	☒	A full description of the statistical parameters including central tendency (e.g. means) or other basic estimates (e.g. regression coefficient) AND variation (e.g. standard deviation) or associated estimates of uncertainty (e.g. confidence intervals)
☐	☒	For null hypothesis testing, the test statistic (e.g. *F*, *t*, *r*) with confidence intervals, effect sizes, degrees of freedom and *P* value noted *Give P values as exact values whenever suitable.*
☒	☐	For Bayesian analysis, information on the choice of priors and Markov chain Monte Carlo settings
☒	☐	For hierarchical and complex designs, identification of the appropriate level for tests and full reporting of outcomes
☒	☐	Estimates of effect sizes (e.g. Cohen's *d*, Pearson's *r*), indicating how they were calculated

Our web collection on statistics for biologists contains articles on many of the points above.

Software and code

Policy information about availability of computer code

Data collection	Agilent OpenLab CDS (C.01.07), BD FACSDiva (8.0.2), Bio-Rad Image Lab (6.0.1)
Data analysis	Microsoft Excel (2019), ImageJ (Version 1.52q)

For manuscripts utilizing custom algorithms or software that are central to the research but not yet described in published literature, software must be made available to editors/reviewers. We strongly encourage code deposition in a community repository (e.g. GitHub). See the Nature Research guidelines for submitting code & software for further information.

Data

Policy information about availability of data

All manuscripts must include a data availability statement. This statement should provide the following information, where applicable:

- Accession codes, unique identifiers, or web links for publicly available datasets
- A list of figures that have associated raw data
- A description of any restrictions on data availability

We have the following statement in the manuscript: "The authors declare that all data supporting the findings of this study are available within the paper, supplementary information files, and source data. Statistical source data for Figures 1-5 and Extended Data Figures 1-5, 7-8, 9d, and 10 are provided with the paper. Uncropped gels and blots for Figure 5 and Extended Data Figures 2, 9 are provided as source data in a Source Data file."

Field-specific reporting

Please select the one below that is the best fit for your research. If you are not sure, read the appropriate sections before making your selection.

☒ Life sciences ☐ Behavioural & social sciences ☐ Ecological, evolutionary & environmental sciences

For a reference copy of the document with all sections, see nature.com/documents/nr-reporting-summary-flat.pdf

Life sciences study design

All studies must disclose on these points even when the disclosure is negative.

Sample size	Sample sizes were n >= 3; this is common practice in the fields of microbial optogenetics (e.g. Ohlendorf et al. J Mol Biol 2012, Jayaraman et al. Nuc Acids Res 2016) and metabolic engineering (e.g. Santos et al. Proc Nat Acad Sci 2012, Liu et al. Nat Comms 2019)
Data exclusions	We did not exclude any data from the analyses.
Replication	All attempts at replication were successful.
Randomization	We did not randomize allocations as statistics were compiled using genetically identical E. coli samples; no human or animal participants were used.
Blinding	Investigators were blinded to group allocation for all experiments except for the bioreactor experiments in Figure 4d, for which data was taken using defined strains/process conditions/illumination scheduling and thus blinding was not possible.

Reporting for specific materials, systems and methods

We require information from authors about some types of materials, experimental systems and methods used in many studies. Here, indicate whether each material, system or method listed is relevant to your study. If you are not sure if a list item applies to your research, read the appropriate section before selecting a response.

Materials & experimental systems

n/a	Involved in the study
☐	☒ Antibodies
☒	☐ Eukaryotic cell lines
☒	☐ Palaeontology
☒	☐ Animals and other organisms
☒	☐ Human research participants
☒	☐ Clinical data

Methods

n/a	Involved in the study
☒	☐ ChIP-seq
☐	☒ Flow cytometry
☒	☐ MRI-based neuroimaging

Antibodies

Antibodies used	-Anti-His tag antibody (HRP), mAb, Mouse (GenScript A00612), Lot: 19K001984 -Anti-LacI antibody [9A5], Mouse (abcam, ab33832), Lot: GR3279941-1 + Goat Anti-Mouse IgG H&L antibody (HRP) (abcam ab205719), Lot: GR3279214-2
Validation	Anti-His tag antibody has been validated by peer-reviewed literature (e.g. Isik et al. PLoS One 2014 https://www.ncbi.nlm.nih.gov/pmc/articles/PMC4172553/). Anti-LacI antibody has been validated by the manufacturer (https://www.abcam.com/laci-antibody-9a5-ab33832.html) as well as peer-reviewed literature (e.g. Purcell et al. J Biol Eng 2012 https://pubmed.ncbi.nlm.nih.gov/22824000/). Anti-Mouse antibody has been validated by the manufacturer (https://www.abcam.com/Goat-Mouse-IgG-HL-HRP-ab205719.html) as well as peer-reviewed literature (e.g. Cai et al. J Cell Biochem 2020 https://pubmed.ncbi.nlm.nih.gov/31190436/).

Flow Cytometry

Plots

Confirm that:

☒ The axis labels state the marker and fluorochrome used (e.g. CD4-FITC).

☒ The axis scales are clearly visible. Include numbers along axes only for bottom left plot of group (a 'group' is an analysis of identical markers).

☐ All plots are contour plots with outliers or pseudocolor plots.

☒ A numerical value for number of cells or percentage (with statistics) is provided.

Methodology

Sample preparation	E. coli samples were diluted 200-fold into 199 uL of ice-cold PBS solution for GFP measurement.
Instrument	LSRII flow cytometer (BD Biosciences, San Jose, CA)
Software	BD FACSDiva 8.0.2
Cell population abundance	10,000 single-cell E. coli events were collected for analysis. Single-cell events comprised 95% of total events for all samples.
Gating strategy	Total E. coli events were visualized and gated by plotting forward vs. side scatter. Single-cell E. coli events were further gated using side scatter area vs. height. GFP gating was set using E. coli strains that either didn't express GFP (negative control) or constitutively expressed GFP (positive control).

☒ Tick this box to confirm that a figure exemplifying the gating strategy is provided in the Supplementary Information.